ITOPF R&D Award 2018
Final Report

ExpOS'D

Experimental Oil Spill Data-sharing

Experimental oil spill

April 16th – April 18th 2019

Marieke Zeinstra	NHL Stenden University of Applied sciences
Corina Brussaard	NIOZ
Terry McGenity	University of Essex
Boyd McKew	University of Essex
Gareth Thomas	University of Essex
Tinka Murk	Wageningen University and Research
Martine van den Heuvel Greve	Wageningen University and Research
Michiel Visser	Rijkswaterstaat Zee & Delta

Acknowledgements

We express thanks to Rijkswaterstaat Zee & Delta, Michiel Visser in particular, for their extensive efforts in organizing this research opportunity. Furthermore, we thank the crew of the involved vessels ARCA, ROTTERDAM and HEBO-CAT 7, as well as the organization providing the aerial surveillance aircraft (Dutch Coastguard, MUMM Belgium, Havariekommando CCME) for their assistance. Furthermore we thank the Belgian authorities (directorate-general Environment of the federal public service health, food chains safety and environment) for the use of their dispersant application equipment.

We thank ITOPF for funding the research activities with the R&D Award 2018. B McKew also acknowledges funding from the Eastern Academic Research council and G Thomas' participation was also supported by The Natural Environmental Research Council EnvEast Doctoral Training Partnership.

Dedication

In memory of Sjon Huisman, whose extensive efforts have been crucial in initiating this experiment.

Contents

Reading Guide

To accommodate for the various nature of the studies performed, the report is divided into different sections:

In chapter 1 the goal of the project and the plans are outlined, as well as the process towards actually performing the experiment.

Chapter 2 describes the experimental oil spill as performed in April 2019 in detail.

In chapters 3 and 4, you'll find a separate chapter per research topic, describing methods, results and conclusions.

1 Introduction

1.1 Description of the project

Like any spill-response option, the goal of dispersant application is to minimize the impacts of the oil. To better predict these impacts and aid decision making, scientists work towards a better understanding of the effectiveness and effects of dispersion of oil under different conditions.
Rijkswaterstaat (the Dutch government agency responsible for oil spill response) has organised an experimental oil spill in the North Sea comparing two different dispersion options (natural and chemical) on separate oil slicks under similar conditions.
The ExpOS'D project was initiated to enable researchers from different international institutes and with different research focus, to collect data from these oil slicks, yielding a uniquely comprehensive and integrated dataset for current and future research. Planned observations included: 1) The behaviour (size, shape, thickness profile) of the different slicks on the water surface over time and spatiotemporal water column hydrocarbon profiles as an indication of the effect of the treatments on the fate of oil and as validation for underlying mechanisms. 2) Analysis of microbial and planktonic community compositions over time, providing an indication of the impact of the treatments on key biogeochemical processes and potential for oil biodegradation. 3) Measurement of concentrations of precursors of aggregate formation (TEP/EPS) to provide insights in the potential of different treatments to induce enhanced marine snow formation or even MOSSFA effects (marine oil-snow sedimentation and flocculent accumulation).
The resulting data-set will be shared publicly to allow a broad application of the obtained data.

1.2 Experimental design

Weather conditions are crucial in this experiment: The wind speed should be at least 5 m/s, to be able to observe the dispersion process (this will not occur with insufficient wind energy). Furthermore, with these conditions, the light oil that is planned for the experiment is expected to disappear on its own without residues. A maximum wind speed of 10 m/s was chosen. Above this wind speed the slicks could disappear too quickly, and the safety during the experiment cannot be guaranteed (especially for sampling with the RHIB).

The project proposal consisted of the following experimental design:
Two dispersant conditions are compared natural dispersion (no treatment) and chemical dispersion (ship based dispersant application). For each of the conditions, two oil slicks are released: one crosswind slick and one into the wind direction. Each slick is a single straight line, released with a controlled outflow from a ship sailing at a fixed speed (Table 1).

Table 1. Slick summaries

	Alpha	*Bravo*	*Charlie*	*Delta*
	Day 1	Day 1	Day 2	Day 2
	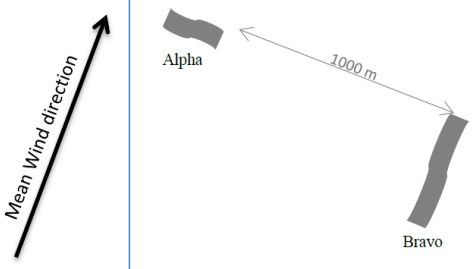		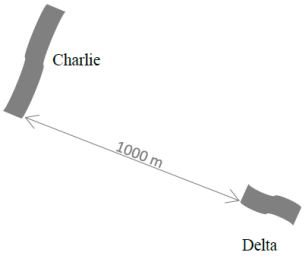	
Oriëntation	Crosswind	Into the wind direction	Into the wind direction	crosswind
Oil Volume	1,5 m^3	3,5 m^3	3,5 m^3	1,5 m^3
Length	215 m	500 m	500 m	215 m
Treatment	None (natural disp.)	None (natural disp.)	Chemical dispersion	Chemical dispersion
	Aerial observation	Aerial observation	Aerial observation	Aerial observation
	Ship based radar	Ship based radar	Ship based radar	Ship based radar
		Sampling oil & water	Sampling oil & water	

After the slicks are deposited, their transport, shape and size are monitored by means of ship-based radar as well as aerial observation.

For the two larger, crosswind, slicks, samples of the oil slick and the water beneath the oil slick are collected at four time intervals, to be analysed for different purposes (Table 2).

Table 2. sampling summary based on original logistics plan (13-04-2018)

Measurement	Institution	Oil Slicks	Locations	Depths	TimePoint	Total number of samples
Water - toxicity test	WUR	Bravo-Charlie	Out -Centre	1,5m-5m	T1-T2	36
Water - phytoplankton pigments (HPLC)	NIOZ	Bravo-Charlie	Out-Edge-Centre	1,5m-5m	T1-T2-T3-T4	48
Water - microbe abundances (FCM)	NIOZ	Bravo-Charlie	Out-Edge-Centre	1,5m-5m	T1-T2-T3-T4	48
Water - nutrients	NIOZ	Bravo-Charlie	Out-Edge-Centre	1,5m-5m	T1-T2-T3-T4	48
Water - zooplankton qualitative analysis	NIOZ	Bravo-Charlie	Out-Edge-Centre	1,5m-5m	T1-T2-T3-T4	48
Water - TEP	NIOZ	Bravo-Charlie	Out-Edge-Centre	1,5m-5m	T1-T2-T3-T4	96
Water- for DNA extraction, qPCR abundance and NGS Miseq amplicon libraries & nutrient analysis	Uessex	Bravo-Charlie	Out-Edge-Centre	surface-1,5m-5m	T1-T2-T3-T4	120
Water - GC/MS hydrocarbon analysis	Uessex	Bravo-Charlie	Out-Edge-Centre	surface-1,5m-5m	T1-T2-T3-T4	192
Oil layer - Dispersant residue	Rijkswaterstaat	Charlie	Centre	surface	T1-T2-T3-T4	8

In addition, laboratory verification experiments are performed with the same oil and dispersant as the field experiment, studying:

- Impact of dispersant on hydrocarbon degradation and microbial communities.
- Formation of Extracellular Polymeric Substances

1.3 Materials

The oil type used was a Light/Medium Arabian Crude (table 3).

Table 3. General properties of the test oil, determined upon first delivery (April 2018)

Name	Method	Units	Result (Temperature)	
Kinematic viscosity	ASTM D445	mm^2/s	10.76 (15 °C)	7.597 (25 °C)
Density	ASTM D5002	kg/m^3	879.4 (15 °C)	872.6 (25 °C)
API gravity	calculated	-	29.32	
Oil-seawater interfacial tension	ASTM D1331	Dynes/cm	14.8 (13 °C)	

Dispersant used was: Dasic Slickgone NS dispersant, from the stock of the Belgian operational spill response organisation.

1.4 Performing the experimental oil spill

The first attempt was planned for April 17th-20th 2018. As weather conditions seemed appropriate, all ships, equipment, materials, observation airplanes and people were mobilized for the execution of the experiment. On the first test day, we sailed out to the test location although expected wind speeds were slightly below optimal. Upon arrival at the test location we were faced with conditions even more quiet than expected, rendering execution of the experiment not useful as well as potentially harmful to the environment due to the persistence of the slick in such conditions. Under the assumption that more suitable conditions might come up in the next days, the equipment and procedures necessary in the experiment were tested.
Later that day, the decision was made to cancel the efforts for this attempt as weather reports did not indicate suitable conditions for the following days.

A new attempt at performing the experiment was planned for September 18th-21st 2018. Our experience during the April attempt was used to make minor adjustment of plans and procedures. Sampling and sample processing procedures were adjusted to adapt to the conditions on board. A separate aerial observations plan was performed to eliminate a centralized briefing with the aircraft crews from different countries and allow them to fly from their home base. However, the weather posed a problem again: due to a tropical storm in the region (ex-hurricane Helene) and the uncertainties in predicting its path, the weather predictions were very uncertain in the week prior to the experiment (at the formal Go/No-go moment).
As a result, the organizers decided to not commence mobilization of ships and materials and cancel this attempt.

The experimental oil spill was performed the third, and final, attempt in April 2019. Because project funds had been lost in (preparations & logistics surrounding) the two previous attempts, the experimental design of the sampling had to be limited.

2 Experimental oil spill April 2019

The third attempt for the experimental oil spill was planned for 16th and 17th of April 2019. As mentioned, some aspects were removed from the sampling plan (table 4).

Table 4. Adjusted sampling plan for April 2019

Measurement	Institution	Oil Slicks	Locations	Depths	TimePoint	Total number of samples
Water - toxicity test	WUR	Bravo-Charlie	Out -Centre	1,5m-5m	T1-T2	36
Water- for DNA extraction, qPCR abundance and NGS Miseq amplicon libraries & nutrient analysis	Uessex	Bravo-Charlie	Out -Centre	surface-1,5m-5m	T1-T2-T3-T4	144
Water - GC/MS hydrocarbon analysis	Uessex	Bravo-Charlie	Out -Centre	surface-1,5m-5m	T1-T2-T3-T4	144
Oil layer - Dispersant residue	Rijkswaterstaat	Charlie	Centre	surface	T1-T2-T3-T4	8

On the day prior to the experiment, we decided to perform a condensed experimental design, as the expected wind speed for the 2nd test day would be insufficient. The condensed plan meant releasing three oil slicks on the same day (Alpha, Bravo and Charlie; table 1), so that the majority of the planned data and observations could still be collected within the 1-day window of suitable conditions.

Table 5. Participants involved in the experimental oil spill in April 2019

Name	Organisation	Role	
Michiel Visser	RWS Zee & Delta	On Scene Commander	ARCA
Bert van Angeren	RWS Zee & Delta	Assistant OCS	ARCA
Marieke Zeinstra	NHL Stenden University of Applied Sciences	Research Leader	ARCA
Sanne Steenbrink	NHL Stenden University of Applied Sciences	Oil deposition obs.	HEBOCAT
Tim Leijssen		Radar Observations	ARCA
Claus van de Weem		Radar Observations	ARCA
Terry McGenity	University of Essex	Principal Investigator	-
Boyd McKew	University of Essex	Principal Investigator Water sampling	ARCA
Gareth Thomas	University of Essex	Water sampling	ARCA
Corina Brussaard	NIOZ	Principal Investigator	-
Anna Noordeloos	NIOZ	Logistics	-
Gianluca Bizzarro	NIOZ	Water sampling	ARCA
Tinka Murk	WUR	Principal Investigator	-
Martine van den Heuvel	WUR	Principal Investigator	-
Vincent Escarvage	WUR	Logistics of samples	-
Eric Donnay	FPS-DG Environment Belgium	Dispersant application	ARCA
Philip Durieux	FPS-DG Environment Belgium	Dispersant application	ARCA
Richard Hill	OSSC	Dispersant application	ARCA
Jon Rees	CEFAS	Modelling	-

2.1 Activities Log

Date	Time (local)	Action
16-04-2019		
	9:00	All ships on site
	9:15	HEBOCAT releases slick Alpha
	9:36	Measurement of environmental conditions (water)
	10:25	HEBOCAT releases slick Bravo
		Sampling outside of slick, T1
	11:12	Measurement of environmental conditions (water)
	11:35	Sampling inside slick Bravo, T1
	11:40	HEBOCAT releases slick Charlie
	12:15-13:17	Dispersant application on slick Charlie
	13:39	Alpha and Bravo slick are merging: Aerial observations indicate initial contact upwind edge of Alpha and downwind tip of Bravo.
	13:46	Sampling inside slick Charlie, T1
	14:13	Measurement of environmental conditions (water)
	14:42	Sampling inside slick Bravo, T2
		Sampling outside of slick, T2
	17:01	Sampling inside slick Charlie, T2
17-04-2019		
	7:52 (5:52 UTC)	EMSA CleanSeaNet detects potential oil slick near original test area. 52° 26' 51" N 003° 50' 44" E
	11:25	ARCA arrives on spill location; The oil slicks have drifted to the shipping lane, some ship trails through them are observed. Small patches of sheen are ominous in the area.
		1st larger slick observed by radar: Shape (long), orientation (East-West) and size (2 km long), give strong indication this is one of the main slicks (either Bravo or Charlie).
	11:41	Measurement of environmental conditions (water)
	11:42	Sampling outside of slick, T3
	11:58	Sampling 1st observed slick, with bottles labelled 'Bravo', T3
	12:12	2nd larger slick observed by radar, to the south of 1st observed slick: Shape, orientation and size, indicate this is one of the main slicks. Distance and orientation towards the other slick (to the south of, and slightly tilted compared to each other) give strong indication that this is the Bravo slick.
	12:23	Sampling 2nd observed slick with bottles labelled 'Charlie', T3
	13:00	Mechanical dispersion/scattering of remaining oil with ARCA
	15:00	Return to port
	19:33 (17:33 UTC)	EMSA CleanSeaNet detects no potential oil slicks in the vicinity of the test location.

The following sub-sections will explain the activities in more detail.

2.1.1 Oil Slick deposition (16-04-18)

Oil was pumped directly out of a tank container on deck of the HEBOCAT 7. To ensure a constant initial thickness within and between slicks, the deposition occurred at a fixed pump-rate (24 m^3/h), with a fixed sailing speed relative to the water (2 knots). The oil was released from a 2"hose, trailing 20 meters behind the ship on flotation bladders, thereby avoiding agitation of the oil slick by the ship itself.

Oil slick Bravo was deposited Northeast of Alpha at that time, at a distance of 2100 m. Crosswind spacing (North-South) was 1000 m, as planned.

Oil slick Charlie was deposited parallel to Bravo, 1500 meters to the North (the spacing was increased based on observed spreading of the existing slicks).

	Deposition start			**Deposition end**		
	Time	**Coordinates**		**Time**	**Coordinates**	
Alpha (crosswind)	09:12			09:18	52°15,129' N	3°59,527' E
Bravo	10:20			10:29	52°14,991' N	3°59,514' E
Charlie	11:34			11:43	52°15,929' N	3°56,520' E

The weight of the container was recorded from the crane on board the ship:

Weight of container+oil before experiment	13,5 tonnes
Weight of container+oil after experiment	8,2 tonnes
Amount of oil deposited	**5,3 tonnes**

With our oil density of 879,4 (15 °C), this means a total of 6,03 m^3 oil was released.

Deposition using the diaphragm pump should be consistent over time, this means slick Alpha is 1,51 m^3 and Bravo and Charlie are 2,26 m^3 each.

2.1.2 Dispersant application (16-04-18)

Dispersant was applied via the ship-borne application system (MARKLEEN Dispersant spray system) installed on the ARCA specifically for this experiment. The dispersant spray arms were fitted on either side of the aft deck. Drop hoses were used to bring the spray nozzles closer to the water surface.

The ARCA sailed through the oil slick with a speed of 3 knots. A constant flow of seawater (110-120 l/min) was maintained through the system. The dispersant flow (9-11 l/min) was started when entering the oil slick and stopped when exiting it. With the sailing speed of 3 knots this would ensure a dispersant dosage of 40 - 50 l per 10 000 m^2 of oiled area, consistent with dispersant manufacturer recommendation.

	Dispersant flow ON			**Dispersant flow OFF**		
	Time	**Coordinates**		**Time**	**Coordinates**	
Track 1 (against the wind)	12:20	52°16,225' N	3°55,643' E	12:28	52°16,668' N	3°56,340' E
Track 2 (with the wind)	12:35	52°16,914' N	3°56,399' E	12:51	52°16,981' N	3°55,190' E
Track 3 (against the wind)	12:59	52°17,188' N	3°55,234' E	13:16	52°18,062' N	3°56,710' E

During the experiment, the dispersant application digital flow meter reading was fairly constant and did not drop below 9 l/min. This would suggest, in the 41 minutes of dispersant application, between 369 and 451 litres of dispersant were applied. However, the calibration of the flowmeter wasn't checked before the experiment and is therefore only indicative. The dispersant used was contained in a standard cubitainer of 600 l. According to the level indications observed at the start (600 l) and end of the experiment (400 l) of the dispersant tank, approximately 200 litres of dispersant were applied on the Charlie slick. This suggests that the values of the flowrate of dispersant indicated by the flowmeter where overestimated. Both values are less than the theoretical recommended maximum amount of (3,5 m^3 x 0,20 = 700 litre).

More spray passes would be advised in case of a real spill situation. For this experiment, it was decided not to do so as it would leave insufficient time for observing the slick behaviour and sampling.

Visually, the dispersion application appeared to work on the treated areas: The treated area seemed clear from oil. However visual observations did not show a visible dispersion effect on the patches of emulsified oil after treatment by dispersants.

For future application of dispersant spray arms on the ARCA, it was advised to fit them more to the front of the ship where the oil film is not pushed away of ship's sides, increasing the oil encounter rate.

2.1.3 Sampling stations

Sampling was performed from the RHIB at three different water depths. Water was sampled at 1,5 and 5 meters below the surface, using a sampling device specialized for sampling beneath floating oil slicks[1]. Surface samples were collected by manually filling a bottle at the water surface .

Label	Notes	Time	Coordinates	
	16-04-19			
Control T1		11:13	52°14'26,6"N	3°59'00,2"E
Bravo T1		11:35	52°14'52,9"N	3°57'17,5"E
Charlie T1		13:46	52°18'56,3"N	3°56'21,3"E
Bravo T2		14:42	52°20'09,7"N	3°57'40,3"E
Control T2		14:56	52°21'01,8"N	3°58'40,5"E
Charlie T2		17:01	52°24'41,3"N	4°01'16,1"E
	17-04-19			
Control T3		11:46	52°25'40,5"N	3°51'30,3"E
Bravo T3	1st observed slick (must be Charlie)	11:58	52°25'23,7"N	3°51'06,2"E
Charlie T3	2nd observed slick, south of first (thus is Bravo)	12:23	52°24'38,7"N	3°49'25,3"E

Oil slick identification on day 2 proved a challenge as a lot of smaller patches were found in the area. After aerial observations guided the ARCA to the most heavily oiled area, the ship-based radar was used to identify oil slicks as 'major' slicks based on expected orientation and elongated shape.

Two major slicks were identified, each around 2 km long, oriented roughly east-west, positioned parallel to one another with a distance of approximately 1,5 kilometres.

Aerial observations for this time confirm these two slicks are the most substantial slicks in the area: They are indicated as the thickest oil observed. Other slick instances identified in the area are a long thin streak of sheen, and spill fragments around the anchorage area.

2.1.4 Measurement of environmental conditions (water)

Using the integrated sensors of the (Seabird) CTD sampler available on board of the ARCA, water column conditions were measured at different times during the experiment.

Used sensors: Temperature (Serial# 1643), Conductivity (Serial# 1443) and Ph (Serial# 0717).

Date	Local Time	Latitude	Longitude	Depth (m)	Temperature (°C)	Conductivity (S/m)	Salinity (PSU)	pH
Apr 16 2019	9:39:38	52,2445	3,9872	1,47	9,08	3,021	27,8	8,4
	11:12:45	52,2370	3,9826	6,96	9,17	3,076	28,3	8,4
	11:17:50	52,2365	3,9794	4,78	9,27	3,014	27,5	8,4

[1] L. Peperzak, P. Kienhuis, C. P. D. Brussaard, and J. Huisman, "Accidental and Deliberate Oil Spills in Europe: Detection, Sampling and Subsequent Analyses," in *Handbook of Hydrocarbon and Lipid Microbiology*, Ed Timmis KN and van der Meer J-R, vol. 78, no. January, Berlin, Heidelberg: Springer Berlin Heidelberg, 2010, pp. 3471–3489.

	14:16:50	52,3245	3,9550	1,31	9,39	3,137	28,7	8,5
	14:18:06	52,3250	3,9553	5,87	8,85	3,438	32,2	8,4
Apr 17 2019	11:47:17	52,4292	3,8544	1,27	9,01	3,514	32,9	8,4
	11:48:49	52,4290	3,8540	4,31	8,93	3,509	32,9	8,4

2.1.5 Radar observations

On board of the MV Arca, a ship-borne oil radar was used to observe the oil slicks in the area around the ship. (Working principle of this radar is similar to that of the SLAR and SAR radars used in aerial and satellite observations: A floating substance can dampen the capillary waves that are normally present on the water surface. The radar picks up the capillary waves and thereby the lack of them is visible as a darker area.) The field of view the first day was roughly 3 km, the second day the wind speed declined and the result was a range of roughly 2 km. The radar operator manually added & edited polygons outlining the slick extent visible on the radar image. The polygons were subsequently saved. Raw data from both days is stored and the operations are summarised as time compressed movie 1 for each day (https://doi.pangaea.de/10.1594/PANGAEA.902609).

The radar image was visible for the crew on board, allowing for the researchers to observe the slicks in real time as well as guiding the ship's crew in operational tasks such as chemical dispersion on day one and mechanically dispersing the remaining slicks on day 2.

2.1.6 Aerial observations

The trials were monitored by different aircraft. A flight schedule was devised to have a continuous view on the oil slick:

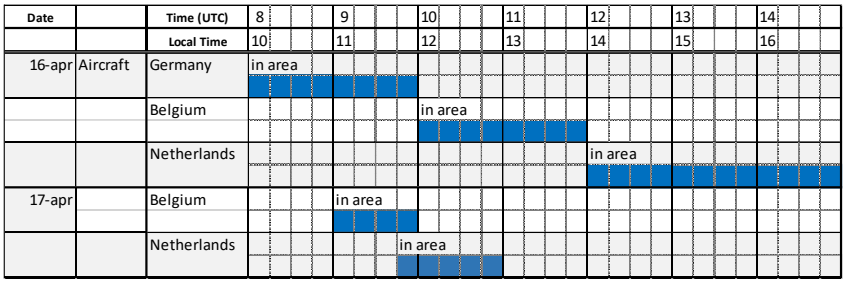

Observers were asked to record oil slick characteristics during the lifetime of the slicks:

- Slick Length
- Slick Width
- Orientation of slick relative to North
- Coordinates of the slick (downwind edge (centre of width))
- Mass distribution within the slick: Is the thickest part down-wind, central, or elsewhere?

In addition, they collected imagery with the different sensors available in the different aircraft (SLAR images, photos, IR/UV images).

2.2 General observations and remarks

The adjustment of the plan to make three of the oil slicks on one day, did have some effect on the data collection:

Not all three slicks could be observed by the oil-radar on the ARCA at the same time as the total size of the test area extended the range of this specific radar. Furthermore, the workload of the sampling crew was high as they had to sample two slicks the same day.

2.2.1 Qualitative observations during the experiment

During dispersant application, the ARCA sailed through the relatively fresh (1-2u) Charlie slick. (Each traverse was through a previously untreated portion of the oil slick.) The participants on board the ARCA had a unique view on this fresh oil layer from the height of the bridge.

- The oil slick was generally thin (metallic), with small irregular streamers of black oil.
- Streamers of light-brown coloured oil were visible within the slick, suggesting emulsification already occurring on this short time-scale.
- Wave breaking in the slick would result in a local clean patch that subsequently gradually built up in thickness through the colours sheen-rainbow-metallic.
- Little black globules of oil were observed in the slick.

3 Research based on the experimental spill

Oil slick elongation and transport as a result of dispersion

Zeinstra-Helfrich M, Marieke

This section describes the behaviour of the oil slicks over time based on observations from the sky as well as the ship based radar. In addition the slick behaviour is compared with oil slick elongation model results.
The oil slicks very clearly elongate in the wind direction, with a rate that is approximately the same for all three slicks, meaning that the crosswind slick Alpha relatively elongates much faster.
The elongation model overestimates the dispersion, thereby making the slicks disappear too quick. The extrapolation of the layer thickness-droplet size relation should be reassessed, as they were not measured for the layer thicknesses that were observed in the field. Furthermore the overestimation of dispersion can partly be attributed to the environmental conditions; the specific situation (wind from over a large landmass) meant the sea was less energetic than our simple wind speed relation predicted.

1. Introduction

One goal of the experimental oil spill was to investigate the manner in which the oil slicks disappear from the water surface over time. Basis of the experiments was comparing the behaviour of 2 long slicks, one of which is placed parallel to wind direction and the second perpendicular to the wind direction. This configuration would allow comparison of the lengthwise dilution process depending on slick size (cross section in wind direction). Furthermore the behaviour of a long wind-wise naturally dispersed slick could be compared with a chemically dispersed slick in the same configuration.

1.1. Theory

Breaking waves submerge local patches of oil. This process (entrainment) occurs at a rate depending on the amount of breaking waves. The submerged oil is broken into droplets with a size dependent on mixing energy, oil properties and oil layer thickness. The droplets rise back to the water surface; their time under the water surface depends on how deep they were entrained (wind speed), density difference between oil and seawater, but mostly on droplet size. As the oil slick is transported by the wind, oil that has been submerged for sufficiently long can resurface upwind of the original slick, causing an elongation (dilution) of the oil slick in the wind direction.

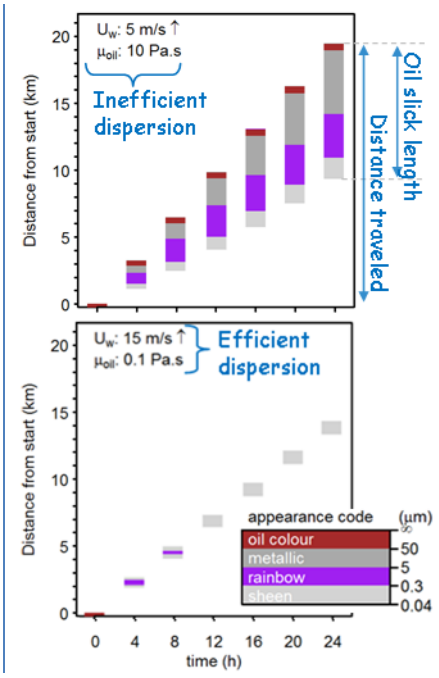

When modelling this phenomenon, two distinct mechanisms show up (Fig. 1):

Fig. 1. Modelled oil slick elongation for two extreme cases. Wind direction is up, colours indicate oil slick thickness, adapted from (Zeinstra-Helfrich et al. 2017)

In case of sub-optimal dispersion, the main slick remains largely intact (in size an thickness) and forms a long tail with decreasing thickness in the upwind direction. Over time, more oil is gradually transported to the tail, which increases in length while the thickness of the main slick very slowly decreases. The downwind edge of the oil slick is displaced in the wind direction with the chosen wind drift factor.

In case of optimal conditions for (natural or chemical) dispersion, a more vertical process occurs. A lot of entrainment is occurring, and entrained oil is broken up into droplets that are very well suspended. As a result, a lot of the oil is moved to the water column in the first hours. As the resulting slick becomes thinner, this process goes increasingly fast. Visible on the water surface is a relatively small oil slick that contains only a small fraction of the original spilled oil. The thickest part of this slick is in de middle, and as most oil is suspended below the surface, the slick movement by wind is much less than the modelled wind drift factor.

For situations between those extremes, a combination of these both processes occurs: in which the slick elongates until the main slick has decreased sufficiently to transition into the vertical behaviour of 'optimal' conditions.

2. Methods

The execution of the experimental oil spill itself has been described in chapters one and two of the main report. This section describes the methods specifically for the investigation of oil slick behaviour and transport.

2.1. Data processing

The observations recorded by the aerial observers (mostly provided in the 'standard Bonn Agreement Pollution forms') were aggregated into one large table.

The oil slick polygons that were collected with the ship-based oil radar, were read & processed using Python. The observations were aggregated into the same table:

- Observation time (corrected from local time to UTC, as well as the 15 minute offset of the radar PC.)
- The polygon itself
- Slick length: length of the polygon's bounding box (The bounding box, is the smallest rectangle that can completely enclose the polygon)
- Slick width: width of the polygon bounding box
- Oiled area: polygon area.
- Orientation: the orientation of the polygon's bounding box, in degrees compared to North.

For slick Alpha, the initial length & width (the first 30 minutes), needed a bit more consideration: The longest axis of the slick (length) is crosswind at the time of deposition and a brief period afterwards, later on the longest axis orients in the wind direction (similar to oil slick B and C). In our analysis we're interested in elongation in the wind-direction, and therefore this is the 'length' we are looking for.

To accommodate this, the characteristics of the first 30 minutes of slick Alpha are calculated separately:

- The width of the slick is the distance between the most Northern and Southern tip of the slick polygon.
- The length of the slick is the distance between the Eastern and Western edge of the slick cross-section in the middle between the North and South tip.

Upon returning to the slicks on the 2nd test day, more oil slick observations were made. These observations are not included in this analysis as the slicks were not undisturbed (they passed shipping).

2.2. Oil Slick elongation modelling

The test conditions were replicated using the Oil Slick Elongation model (Zeinstra-Helfrich et al. 2017).

- Slick Alpha & Bravo were modelled from (just after) deposition: using length as observed at that time & oil volume/slick area as thickness.
- Slick Bravo & Charlie were modelled starting 1,5 hour after deposition (the time chemical dispersion was finished). The simulations use length as observed at that time & oil volume/slick area as thickness.

		A	B	B > 1,5 h	C > 1,5 h
L_0	m	241	1067	2019	1851
H_0	m	1,26E-05	3,68E-05	3,31E-06	4,37E-06

Oil properties of the fresh oil were based on the measurements as performed in April 2018. Oil properties of weathered oil were based on weathering calculations for an amount of 3,5 m^3 of our oil for 1,5 hours.

		Fresh	Weathered	Weathered + dispersant
ρ_{oil}	kg/m^3	879,4	937	937
μ_{oil}	Pa.s	9,46E-03	2,21E-01	2,21E-01
$\sigma_{oil\text{-}sw}$	N/m	0,0148	0,0148	0,00148

The model was run with different settings for wind speeds. (7,5, 8,9 and 6,5 m/s)

3. Results

The data table of oil slick observations is stored available via PANGAEA (https://doi.pangaea.de/10.1594/PANGAEA.902311). The data was used to produce images per oil slick. In this chapter we describe the results, the images can be found in the appendix (pages 24 to 28).

3.1. General observations on the slick behaviour over time

Slick *Alpha* (p24-25)was deposited at 7:12u UTC, and can only be observed for a little over 5 hours before merging with Bravo. It was deposited across the wind: On the first radar observation, 13 minutes after deposition, its angle is 29° compared to North. The Alpha slick very clearly develops a tail in the upwind direction (east). As a result, the longest axis soon shifts towards an orientation around 90°.

From 9:30, the aerial observers consistently report a greater oil slick length than the ship-based radar. The mismatch appears to occur in pinpointing the western tip of the oil slick. As the ARCA was sailing near slick Bravo at that time, the western tip was our far side: there is a possibility we underestimated the western tip of slick alpha as it neared the edge of the radar range. Oil slick width observations show better agreement between aerial reporting and radar observations.

The (crosswind) width of the slick gradually increases from just below 0,5 km to 1,21 km. The length (in wind direction) of increases up to 3,700 km in 4,32 hours. This is an increase of 3,5 km compared to the first observed length of 215 meters.

The IR images made by the German Coastguard over a period of two hours (8-10 UTC) very clearly show a thick 'streak' in the downwind edge of the oil slick. The thick portion starts off as a 50-100 m wide crosswind band, visible 1 hour after deposition (IR image 8:16UTC), developing a progressively longer tail over time (Fig. 13, p25). The thick portion slowly appears to decrease in thickness and size.
Subsequent aerial observations by the Belgian Coastguard record the same phenomenon: at 10:32 and 11:15 they record a long slick oriented around 90°, with the thickest portion at or near the downwind edge. In their final observation (11:44), no specific thickest part can be observed and the slick area is 60% sheen and 40% metallic (Fig. 12, p24).

Slick *Bravo* (p26-27) was deposited at 8:25 UTC, into the wind direction (69° compared to North). The orientation quickly shifts to 80° and remains so fairly constant.

In the first 3 hours of the slick lifetime, radar and aerial observations of length, width and location are in good agreement. After 12 UTC, it is presumed that the aerial observers included the former slick Alpha in their observations of slick Bravo. There is a big jump in slick length, width and area at that time, largely consisting of sheen- oil thicknesses (0,04 – 0,30 µm).

Slick bravo starts of 212 meter wide and spreads to 1518 m wide. Ship-based radar observations, indicate length increased from 1,02 to 5,26 km in 6,79 hours (for comparison with Alpha: Bravo elongates to 3,44 km in 4,29 h).

The thick part of slick Bravo is an elongated wind-wise shape: In the IR images of 9:15, 9:35 and 9:59, the thick portion of slick Bravo is 1,3 to 1,4 km long, and a thinner sheen is forming on the upwind (right) side. Subsequent Aerial observations (10:36, 11:13), indicate the thick portion on the downwind side in the form of an elongated shape of 1,3 and 1,5 km long (reported as the downwind 50% of the 2,6 km long slick, the downwind 50% of the 3,0 km long slick respectively). In the last observation (11:48), the thick portion has an undefined length and is positioned at 30% of the slick length.

Thickness observations until 12:00 UTC indicate show the slick is spreading out: The area of thickest oil (true oil colour, class 4&5) decreases, while area of the thinner oil increases. (After 12 UTC, this graph is affected by slick Alpha.)

Oil slick *Charlie* (p28) was deposited at 11:34 UTC, dispersants were applied over the period 10:20 - 11:16 UTC. The initial orientation the slick was 55°, the angle increases to 65-70°, but settles down around 55° at the end of test day 1.

Radar and aerial observations of oil slick length match very well for slick Charlie. There is some disagreement between the width observations, however. This could be due to the generally irregular shape of the oil slick. (The polygons show more 'jagged' edges, compared to the 'smoother' slick Bravo).

Slick Charlie spreads from 117 meter to 951 meter in width. The length increases from 878 meters to 4,20 km in 5,51 hours. (In 4,32 and 4,38 hours the slick elongates to 3,89 km (Ship Radar) and 3,30 km (Aerial observation)).

Thickness observations of slick Charlie are a bit less clear than for the other slicks, in part because IR observations were no longer available at that time. Aerial observations indicate the thickest portion of the slick to be in the centre of the width, subsequently:

- in 3 patches, starting at 30% of slick length (10:38)
- from start until width of the slick (11:13)
- at 40% of length starting downwind (11:42): 40% of 2,6 km long = 1,3 km long.

Slick Charlie spreads out: over time, the area of thinner slick (sheen, rainbow & metallic) increases while the true oil colour decreases.

3.2. Model results

The initial model runs were based on wind speed of 7,5 meters per second and oil thicknesses based on observations. The outputs of these runs (Fig. 4 and Fig. 5, page 21), clearly show the behaviour of the oil slicks matches that for very efficient dispersion (favourable conditions): the oil slick length does not increase very much, the thick part remains central to the slick.

The models were run with some variations of inputs (wind speed & oil thickness) to investigate to what extend a better match with observations can be obtained. In order to easily compare different model results with the observed behaviour of the oil slicks, we've plotted visible oil slick length over time as observed (coloured markers) versus the different model outputs (lines) in Fig. 6, page 21. As expected, a lower wind speed and a higher oil layer thickness result in less efficient dispersion and a larger slick length.

To check the intermediate calculations in the model, like wave height, breaking wave coverage etc., we've looked up observed values during our test period:

- Unfortunately, the calculated white-cap coverage cannot be compared with satellite obtained white cap coverage (Salisbury *et al.*, 2014) as wind-sat overpasses did not match our test-times and locations.
- Measured significant wave heights near the test site (Fig. 3, page 20) only briefly reach up to 90 cm, but are mostly below that value. The model does calculate higher wave heights at the wind speeds used as input (Tab. 1, page 20).

4. Discussion

All methods combined, a great number observations were made of the oil slicks.

For the radar observations, the vicinity to the oil slick was crucial in capturing the outlines of the slicks correctly. Differences between aerial observations and radar observations indicate the 'far side' of the oil slick was not always captured correctly, especially if the ARCA was a bit further off (the radar observations of slick Alpha after 9:00 UTC). At the end of the first test-day the ARCA performed an extra transect of the entire slick-length between slick Bravo & Charlie, to completely capture their outlines at this time.

The aerial observations vary with time, based on the sensor techniques available on the aircraft, as well as on the 'experience' of the crew with these oil slicks.

The observations of slick Alpha & Bravo are most clear, partly because of the available sensor systems at that time, and partly because they were observed for the longest period of time. Unfortunately the merging of the slicks didn't allow for longer comparison of their behaviour.

Observations of slick Charlie were a little less abundant. It could only be observed 'unobstructed' for a brief period: Deposition of this slick was last in the row, and applying dispersants took quite some time. Furthermore, at that time, IR observations which have proven very valuable in analysing the other slicks, were no longer available. Of course, the three transverses of the ARCA through the slick for dispersant application probably affected the slicks behaviour and may have caused some additional scattering.

Model results

The model results overestimate the dispersion compared to what was observed. Of course, the elongation model is a simplification of reality and only considers the mechanism of dispersion over a lengthwise cross-section.

The oil slick elongation model is very sensitive to layer thickness, as this parameter influences the droplet size distribution. With input of a layer thicknesses realistic in this field exercise, the slick disappears too quickly. This means that the extrapolation of the droplet size calculations to these minute thicknesses should be re-assessed.

The significant wave height as measured at a representative location, is much lower than the significant wave height the model calculates for the observed wind speed. Of course, in reality, wave generation is much more complex than our parameterization with wind speed only. The wind direction from the east (from across the European land mass) meant that there has not been much room for wave build-up. This could explain the lower significant wave height and can indicate the conditions were less energetic than the wind-speed parameterizations in the model predict.

Slick behaviour

The observations of oil slick behaviour support the theory of an oil slick elongating (diluting) in the wind direction. The thick portion of both slicks Alpha and Bravo remains downwind and largely the same size, while the length of the oil slick increases trough a thinner tail upwind.
The oil slick initial orientation had a very big influence on the elongation of the slick. (Note that all three slicks were deposited with the same speed of sailing and pump-speed, and therefore an equal initial thickness.) The cross-wind slick (Alpha), despite its smaller volume and initial length, becomes just as long as the other slicks in the same timeframe. This means that the (absolute) increase in length in the wind direction on this time-scale was roughly the same for the slicks, indicating that the elongation of the oil slick happened at a fixed rate (for these conditions and oil properties) and was not affected by initial length. For all three slicks, ignoring suspicious measurements, the increase in length occurs approximately the same rate from the start to the end of the observation period.
Relatively, the elongation of slick Alpha is much larger. As a result, the thick portion of the slick is visibly declining and disappears altogether in the end. This suggests that his slick is successfully 'diluting' by elongation and would disappear later on.

The theory that the downwind portion of the slick feeds the tail is further supported by the observation that a thickness gap in the slick Alpha, is translated down the entire slick tail length: In the thick downwind edge of slick Alpha, a thinner region can be seen in the IR images (Fig. 13, p25). Over time, the upwind tail of this region remains slightly thinner than the remainder of the tail.

5. References

Alzarhani, A.K., Clark, D.R., Underwood, G.J.C., Ford, H., Cotton, T.E.A., and Dumbrell, A.J. (2019) Are drivers of root-associated fungal community structure context specific? *ISME J* **13**: 1330–1344.

Auguie, B. (2017) gridExtra: functions in Grid graphics. R Package Version 2.3. *CRAN Proj*.

Becker, R.A., Wilks, A.R., Brownrigg, R., Minka, T.P., and Deckmyn, A. (2016) Package "maps": Draw Geographical Maps. *R Packag version 23-6*.

Bodenhofer, U., Kothmeier, A., and Hochreiter, S. (2011) Apcluster: An R package for affinity propagation clustering. *Bioinformatics* **27**: 2463–2464.

Clark, D.R. (2019) ecolFudge.

Coulon, F., McKew, B.A., Osborn, A.M., McGenity, T.J., and Timmis, K.N. (2007) Effects of temperature and biostimulation on oil-degrading microbial communities in temperate estuarine waters. *Environ Microbiol* **9**: 177–186.

Dumbrell, A.J., Ferguson, R.M.W., and Clark, D.R. (2016) Microbial Community Analysis by Single-Amplicon High-Throughput Next Generation Sequencing: Data Analysis – From Raw Output to Ecology. In *Hydrocarbon and Lipid Microbiology Protocols*. McGenity, T.J., Timmis, K.N., and Nogales, B. (eds). Berlin, Heidelberg, Heidelberg: Springer Protocols Handbooks, pp. 155–206.

Edgar, R.C., Haas, B.J., Clemente, J.C., Quince, C., and Knight, R. (2011) UCHIME improves sensitivity and speed of chimera detection. *Bioinformatics* **27**: 2194–2200.

Field, D., Houten, S., Thurston, M., Swan, D., Tiwari, B., Booth, T., and Bertrand, N. (2006) Open software for biologists: from famine to feast. *Nat Biotechnol*.

Joshi, N. and Fass, J. (2011) sickle - A windowed adaptive trimming tool for FASTQ files using quality. *(Version 133)* [Software].

Klindworth, A., Pruesse, E., Schweer, T., Peplies, J., Quast, C., Horn, M., and Glöckner, F.O. (2013) Evaluation of general 16S ribosomal RNA gene PCR primers for classical and next-generation sequencing-based diversity studies. *Nucleic Acids Res* **41**: 1–11.

Lozada, M., Marcos, M.S., Commendatore, M.G., Gil, M.N., and Dionisi, H.M. (2014) The Bacterial Community Structure of Hydrocarbon-Polluted Marine Environments as the Basis for the Definition of an Ecological Index of Hydrocarbon Exposure. *Microbes Environ* **29**: 269–276.

McKew, B.A. and Smith, C.J. (2015) Real-Time PCR Approaches for Analysis of Hydrocarbon-Degrading Bacterial Communities. In *Hydrocarbon and Lipid Microbiology Protocols*. McGenity, T.J., Timmis, K.N., and Fernandez, B.N. (eds). Berlin, Heidelberg: Springer Protocols Handbooks.

Nikolenko, S.I., Korobeynikov, A.I., and Alekseyev, M.A. (2013) BayesHammer: Bayesian clustering for error correction in single-cell sequencing. *BMC Genomics* **14**:.

Nurk, S., Bankevich, A., Antipov, D., Gurevich, A., Korobeynikov, A., Lapidus, A., et al. (2013) Assembling genomes and mini-metagenomes from highly chimeric reads. In *Lecture Notes in Computer Science (including subseries Lecture Notes in Artificial Intelligence and Lecture Notes in Bioinformatics)*. pp. 158–170.

Pedersen, T.L. (2019) patchwork: The Composer of Plots. *Cran*.

R Development Core Team, R. (2011) R: A Language and Environment for Statistical Computing.

Rognes, T., Flouri, T., Nichols, B., Quince, C., and Mahé, F. (2016) VSEARCH: a versatile open source tool for metagenomics. *PeerJ* **4**: e2584.

Salisbury, D.J., Anguelova, M.D., and Brooks, I.M. (2014) Global distribution and seasonal dependence of satellite-based whitecap fraction. *Geophys Res Lett* **41**: 1616–1623.

Searle, S.R., Speed, F.M., and Milliken, G.A. (1980) Population marginal means in the linear model: An alternative to least squares means. *Am Stat* **34**: 216–221.

Tatti, E., McKew, B.A., Whitby, C., and Smith, C.J. (2016) Simultaneous dna-rna extraction from coastal sediments and quantification of 16S rRNA genes and transcripts by real-time PCR. *J Vis Exp* **2016**: e54067.

Venables, W.N. and Ripley, B.D. (2002) Modern Applied Statistics with S (Fourth Edition).

Wang, Q., Garrity, G.M., Tiedje, J.M., and Cole, J.R. (2007) Naïve Bayesian classifier for rapid assignment of rRNA sequences into the new bacterial taxonomy. *Appl Environ Microbiol* **73**: 5261–5267.

Wang, W., Wang, L., and Shao, Z. (2010) Diversity and Abundance of Oil-Degrading Bacteria and Alkane Hydroxylase (alkB) Genes in the Subtropical Seawater of Xiamen Island. *Microb Ecol* **60**: 429–439.

Zeinstra-Helfrich, M., Koops, W., and Murk, A.J. (2017) Predicting the consequence of natural and chemical dispersion for oil slick size over time. *J Geophys Res Ocean* **122**: 7312–7324.

6. Appendix:

6.1. Environmental conditions

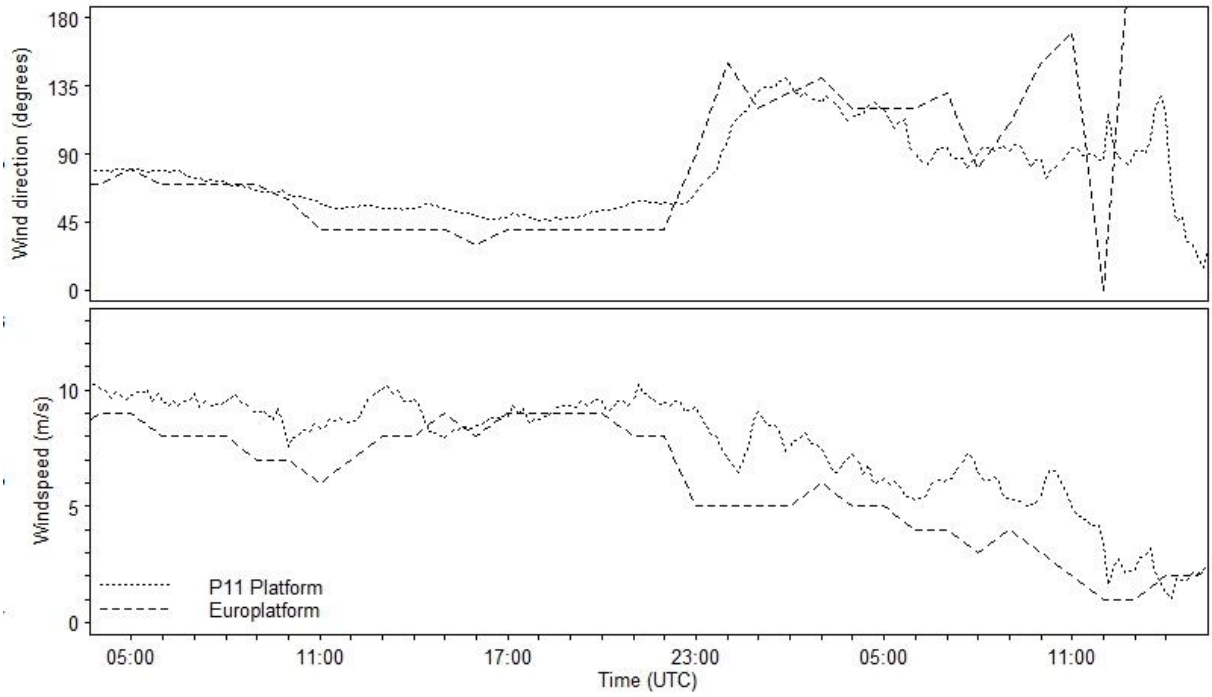

Fig. 2. Wind speed during the first test day, as observed by 2 offshore stations. (P11 platform position is 3,342°E, 52,359°N, 45 kilometres Northwest of our test site. Europlatform position is 3,275°E, 51,998°N, 55 kilometres Southwest of our test site.) Data downloaded from https://waterinfo.rws.nl/#!/nav/index/ and https://www.knmi.nl/nederland-nu/klimatologie/uurgegevens_Noordzee.

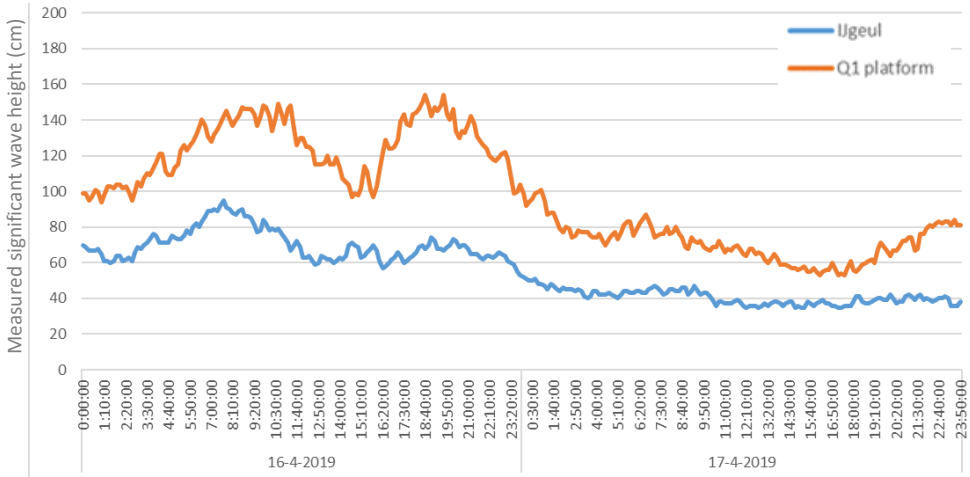

Fig. 3. Significant wave height measured at station 2 stations: Bleu line: 'IJgeul 1' Position of this station: 4,264°E, 52,488°N, located 31 km Northeast of our test position. Orange line 'Q1 platform', position 4,150°E, 52,925°N, located 75 km North northeast of our test site.
Distance from the coast: test site: 24,1 km, IJgeul1: 21,1 km, Q1 platform: 55,2 km.

Wind speed (m/s)	Significant wave height (m)
5,0	0,6
5,5	0,7
6,0	0,8
6,5	0,9
7,0	1,1
7,5	1,3
8,0	1,4
8,5	1,6
9,0	1,8

Tab. 1. Significant wave height as calculated by the model for each wind speed.

6.2. Model results

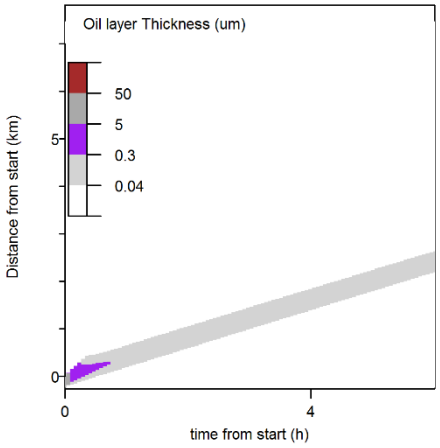

Fig. 4. Model output, slick Alpha. Wind speed 7,5 m/s (upwards)

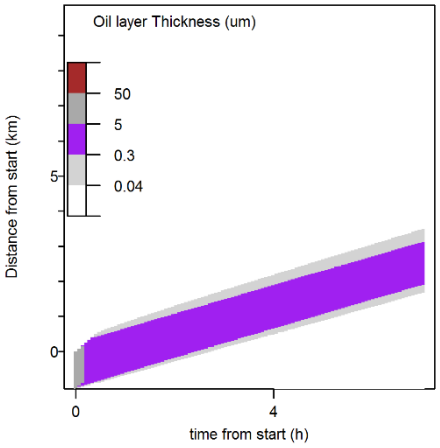

Fig. 5. Model output, slick Bravo. Wind speed 7,5 m/s (upwards)

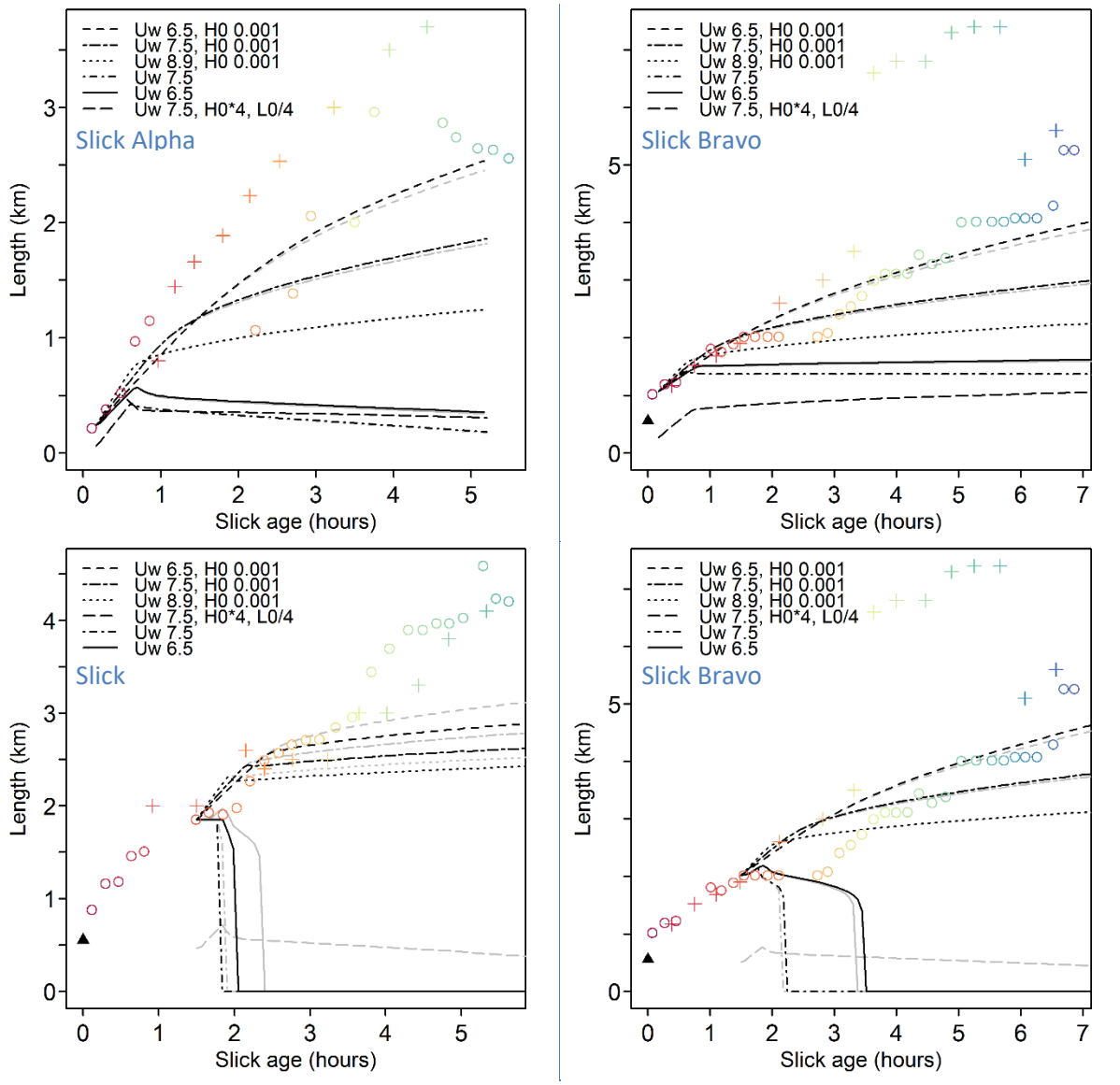

Fig. 6. Combined elongation model output (lines) compared to slick observations (markers) of oil slick length. Black lines are simulations based on un-weathered oil properties, grey lines are simulations based on weathered oil properties. Other model settings are given in the legend: wind speed (Uw in m/s) and layer thicknesses H0 in meters, if other than originally planned.

6.3. Appendix: Oil slick observations

Slick alpha and Bravo merging

The aerial observation images indicate initial contact between slick Alpha and Bravo took place between 11:23 and 11:48 (Fig.1 & Fig.3).

Using the ship based radar, the slick extent of Alpha and Bravo were recorded separately until 12:47 UTC (Fig.2). Because the operator had followed both slicks during their lifetime, he could distinguish the wider shape of A from the narrower, longer shape of B.

The aerial observers recorded slick data for Alpha and Bravo separately until 12:00 UTC. The new aerial observations crew starting at 12:00 UTC could not distinguish the different slicks (Fig.4 & Fig.5).

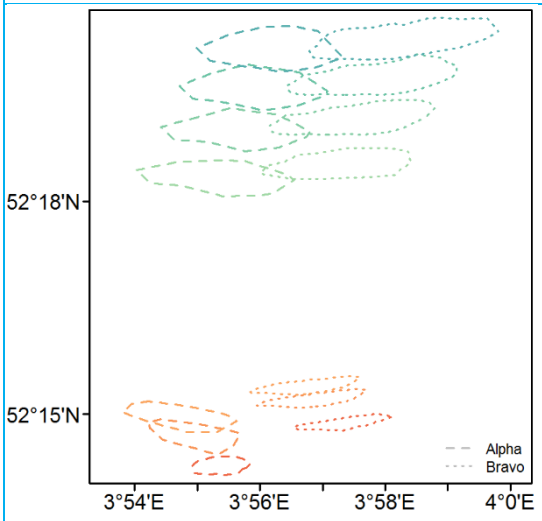

Fig. 8. Slick outlines obtained from the ship based radar. For each of the 7 time points (colour) a set of both Alpha and Bravo is shown (line types).

Fig. 7. 11:23 UTC. slick Bravo in the foreground, slick Alpha on the left hand border, slick Charlie in the background (right).

Fig. 9. 11:48 UTC: slick Alpha in the foreground. In the background slick Charlie (left) and Bravo (right)

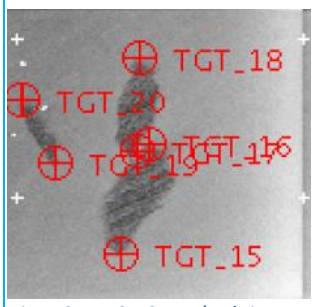

Fig. 10. 11:34 SLAR (Belgium CG).

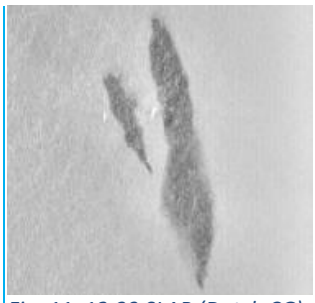

Fig. 11. 12:39 SLAR (Dutch CG)

In both these SLAR images: Slick Charlie to the left. On the right hand side, slick Alpha (bottom) connected to slick Bravo (top)

Individual oil slick observations

The following pages contain an overview of the observations of each oil slick. These consist of a combination graph of the characteristics the slick. The graph layout is as follows:

<table>
<tr><td>Name of the oil slick</td><td rowspan="2">Graphs on the left hand side for the evolution of characteristic oil slick properties over time.
Symbols indicate observation types. From top to bottom:
- Slick length: The longest axis of the slick, as reported on the observation forms (aerial observation) or calculated from the polygons.
- Oil Slick width: The shortest axis of the slick, as reported on the observation forms (aerial observation) or calculated from the polygons.
- Total oil slick surface area.
- Surface area of the oil slick in each of the Bonn Agreement Colour Codes (obtained from aerial observations only)
- Oil slick orientation, in degrees compared to North.</td></tr>
<tr><td>Legend: Across the graph:
Colours indicate the slick age since deposition, ranging from red to blue.
Symbols indicate the type of observation.</td></tr>
<tr><td>The large graph on the right hand side, shows slick extent & position over time:
- Radar observations of the slick outline are plotted as polygons.
- Symbols (x and +) connected by dotted lines are the starting & end positions coordinates of the slick as reported by the aerial observations crew. An additional (◊ or □) on the same line, indicates the position of the thickest part inside the slick.</td><td></td></tr>
<tr><td></td><td>In the small box on the bottom right, significant timing information is given:
For slick A & B, three vertical lines indicate timing of their merger: 11:48 confirmed contact; 12:00u final aerial observation that considers them separate; 12:47 final separate radar observation</td></tr>
</table>

In addition, some characteristic images of the oil slick are provided. For all images, see https://doi.pangaea.de/10.1594/PANGAEA.902608.

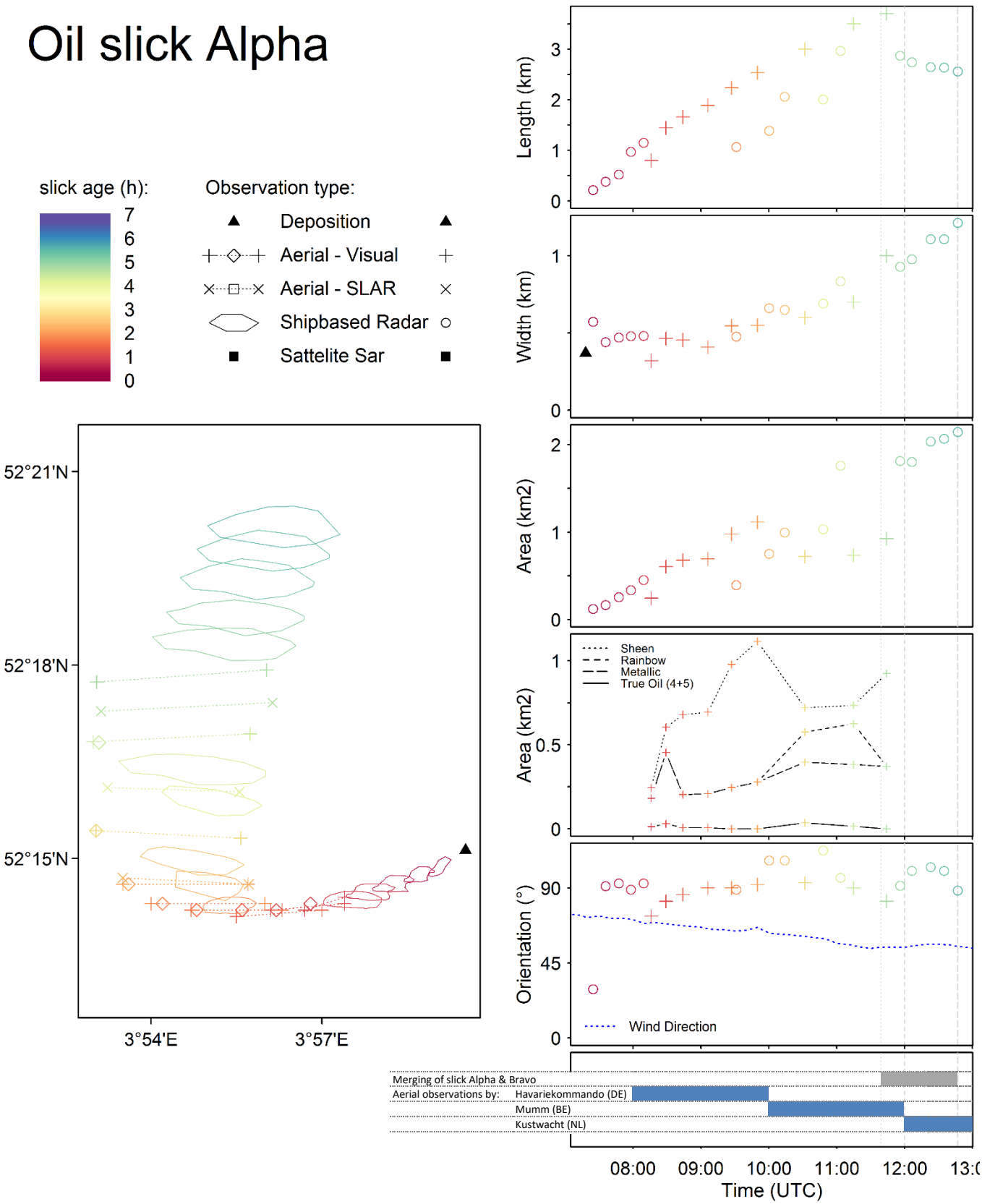

Fig. 12. Combined plot of all observations of slick Alpha over time.

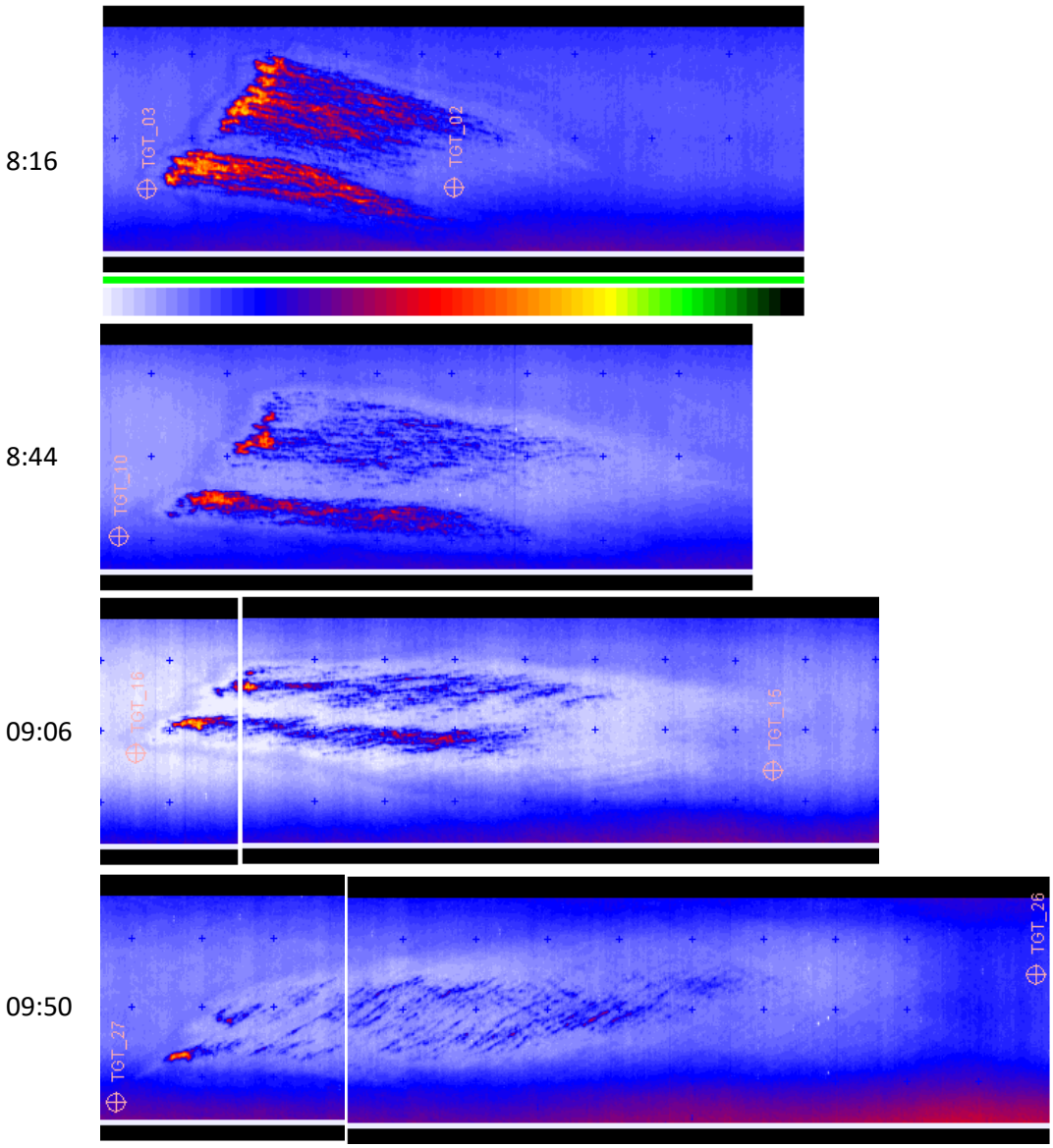

Fig. 13. IR images of slick Alpha, at different time points, made by the German Coastguard. Grid: 200 m

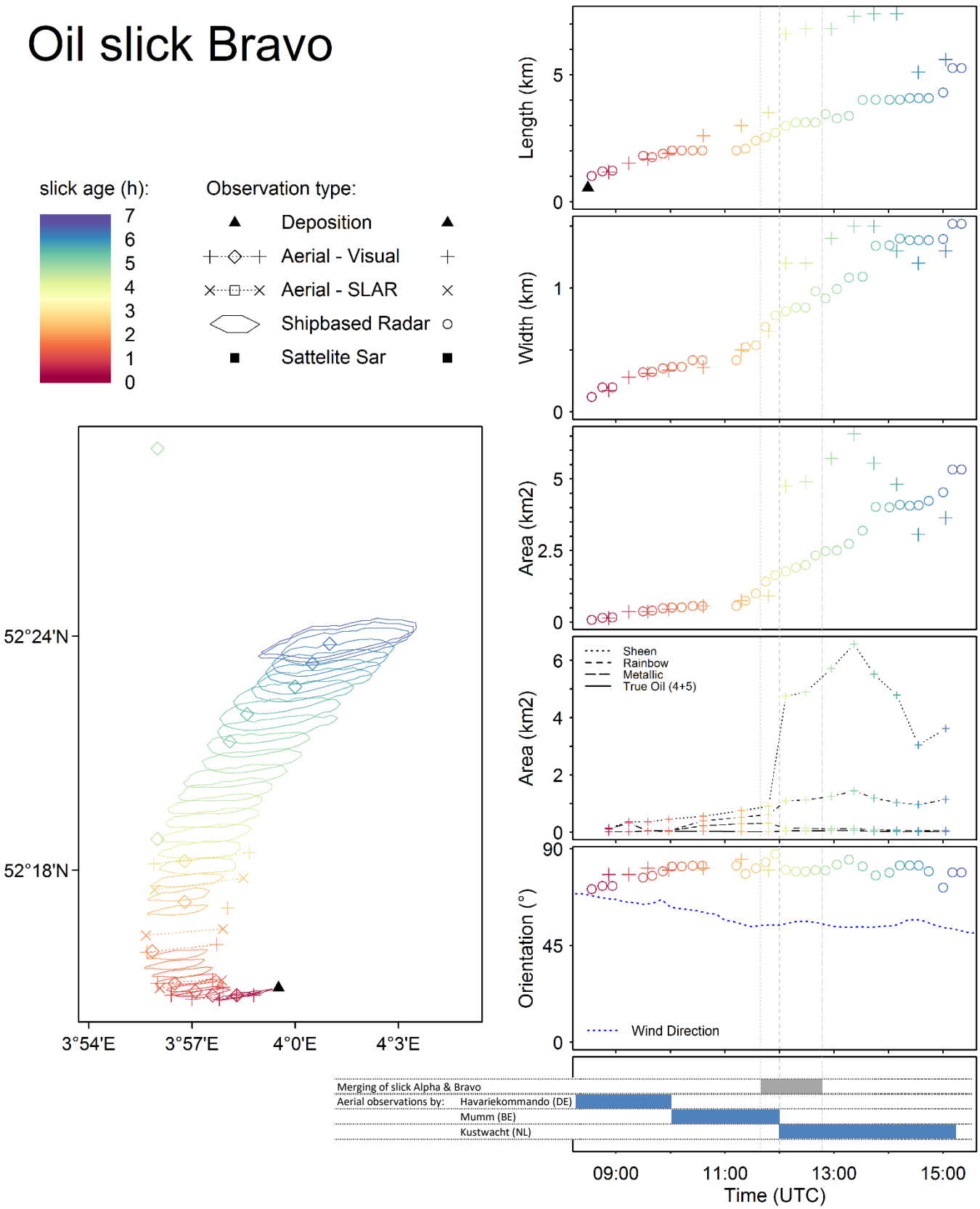

Fig. 14. Combined plot of all observations of slick Bravo over time.

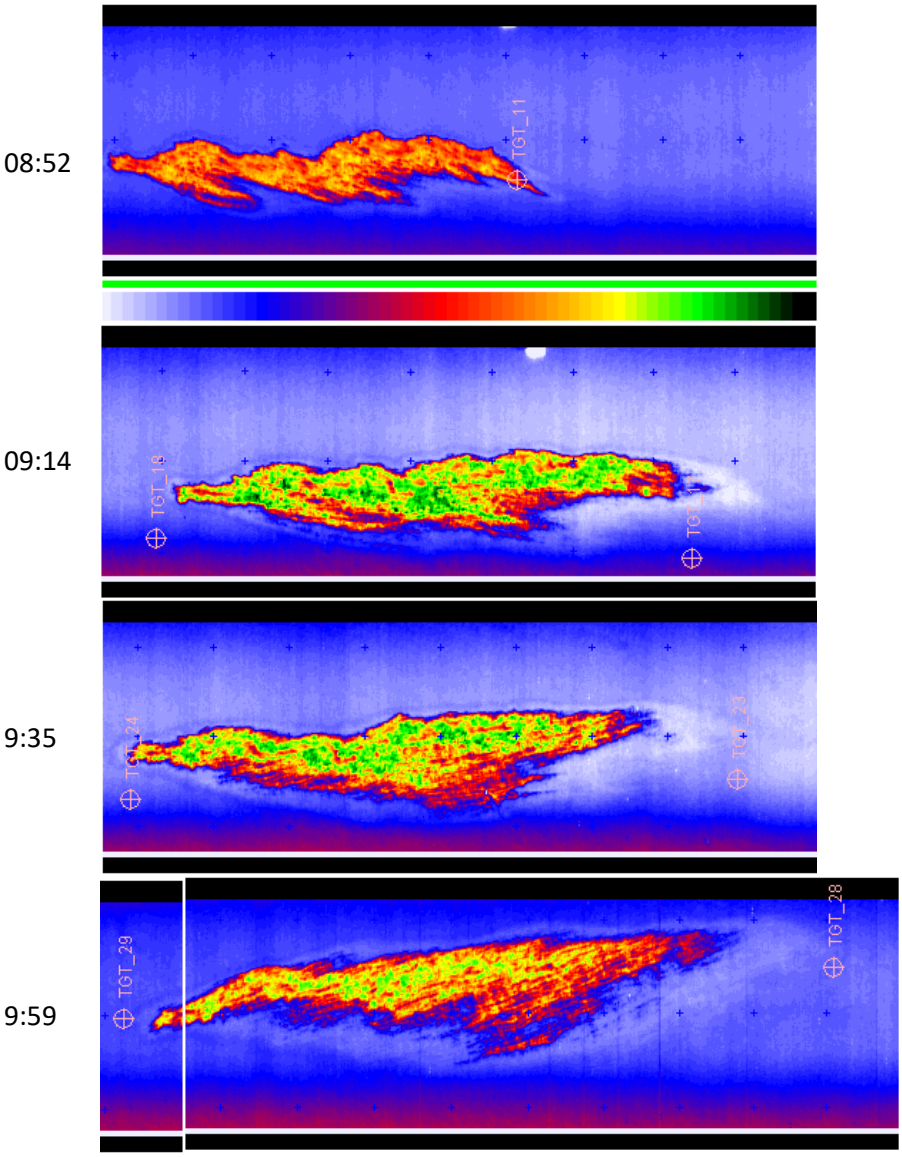

Fig. 15. IR images of slick Bravo, at different time points, made by the German Coastguard. Grid: 200 m

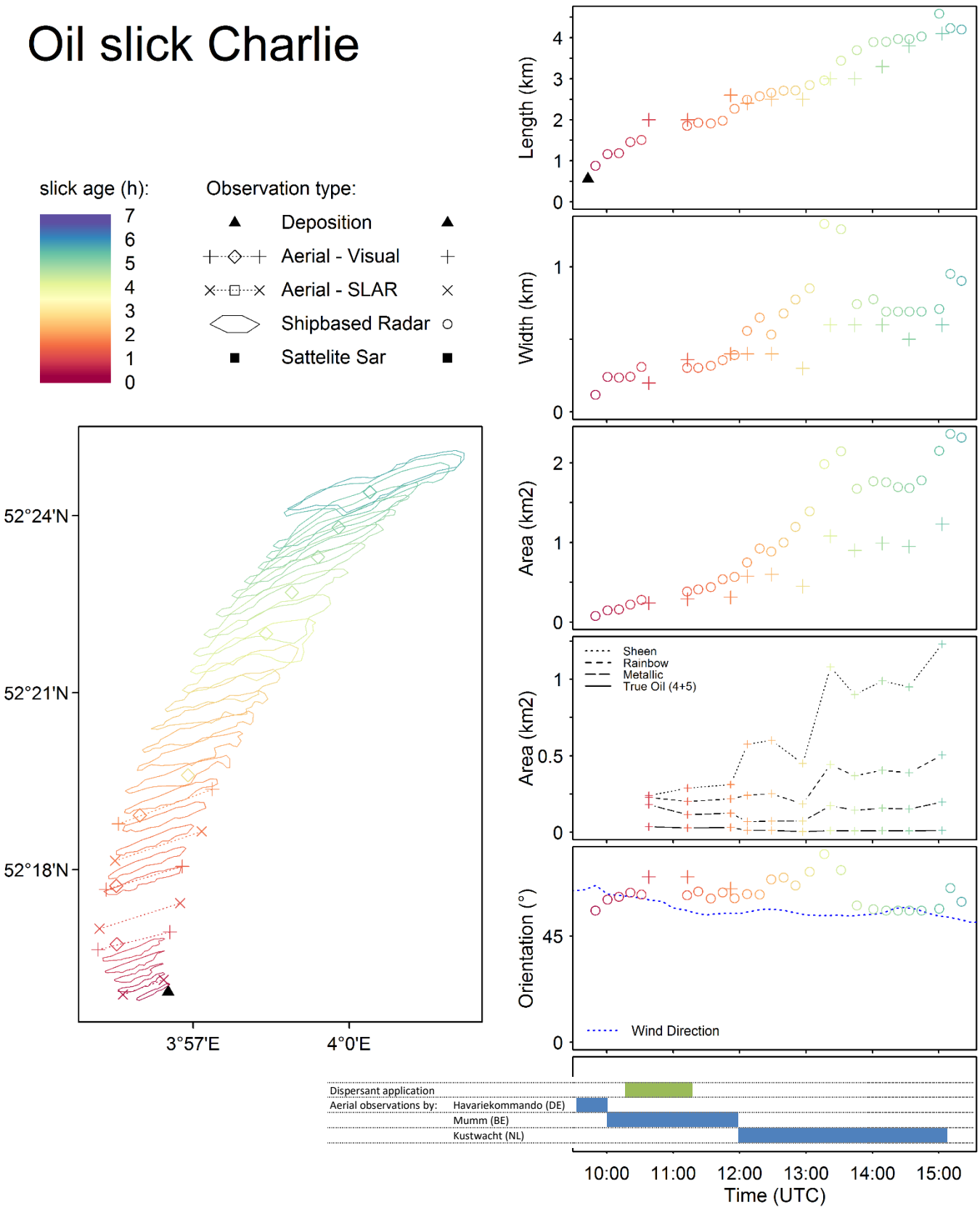

Fig. 16. Combined plot of all observations of slick Charlie over time.

Chemical vs Natural Dispersion: Impacts on microbial communities and hydrocarbon biodegradation

Thomas, Gareth; McGenity, Terry J; McKew, Boyd A

Materials & Methods

These methods describe what will be (and some have been) taking place on the ExpOS'D samples and are therefore subject to slight alterations where required.

Nutrient Analysis

Nutrient analysis was conducted on all samples to determine concentrations of ammonia (NH_{4+}), phosphate ($PO4_{3-}$), silicate (SiO_{2-}), nitrate (NO_{3-}), and nitrite (NO_{2-}). Ammonia concentrations were measured by protocol G-327-05 Rev.6, phosphate by protocol G-297-03 Rev.5, silicate by protocol G-177-96 Rev.10, and nitrate and nitrite via protocol G-172-96 Rev.13 on a SEAL Analytical AA3 HR AutoAnalyzer tandem JASCO FP-2020 Plus fluorescence detector.

Hydrocarbon Degradation

Hydrocarbons were extracted from 50 ml brown-glass vials (collected *in situ*) using a 6 ml solvent extraction of 1:1 hexane and dichloromethane, vigorously shaken for 30 seconds, and placed in an ultrasonic bath for 30 minutes. Deuterated alkanes (nonadecane $C_{19}d_{40}$ and triacontane $C_{30}d_{62}$ at 10 µg ml^{-1}) and PAH (naphthalene-d_8 and anthrancene-d_{10} at 10 µg ml^{-1}) internal standards were added to each sample and quantification was performed on an Agilent 7890A Gas Chromatography system coupled with a Turbomass Gold Mass Spectrometer with Triple-Axis detector, operating at 70 eV in positive ion mode, using conditions as previously described by Coulon *et al.*, (2007). External multilevel calibrations were carried out using alkanes (Standard Solution (C^8-C^{40}); Sigma), methylated-PAHs (1-methylnapthalene, 2-methylanthracene, and 9,10-dimethylanthracene; Sigma), and PAH (QTM PAH Mix; Sigma) standards, the concentrations of which ranged from 1.125 to 18 µg ml^{-1}. For quality control, a 2.0 ng l^{-1} diesel standard solution (ASTM C12-C60 quantitative, Supelco) and a 1.0 ng l^{-1} PAH Mix Standard solution (Supelco) were analysed every 15 samples. The variation of the reproducibility of extraction and quantification of water samples were determined by successive extractions and injections (n = 6) of the same sample and estimated to be ± 8%. All alkanes between C_{10} and C_{36} including pristane and phytane and the following PAHs were quantified (naphthalene; all isomers of methyl-, dimethyl- and trimethyl-naphthalenes; acenaphthylene; acenaphthene; fluorine; phenanthrene; all isomers of methyl- and dimethyl-phenanthrenes/anthracenes; fluoranthene; pyrene; all isomers of methyl- and dimethyl-pyrene; chrysene; all isomers of methyl- and dimethyl-chrysene). Only those hydrocarbons detected are shown in Fig. 6.

qPCR analysis of Bacterial 16S rRNA genes

DNA was extracted from *in situ* seawater samples from the thawed Millipore® Sterivex™ filters with a DNeasy PowerWater Sterivex Kit (Qiagen) according to the manufacturer's instructions. The primers used for quantification of bacterial 16S rRNA were 341f - CCTACGGGNGGCWGCAG and 785r – GACTACHVGGGTATCTAATCC (Klindworth *et al.*, 2013). qPCR reactions were performed using a CFX384™ Real-Time PCR Detection System (BioRad) with a PCR using reagents, cycle conditions, and standards as previously described (McKew and Smith, 2015; Tatti *et al.*, 2016). Inspection of standard curves showed that all assays produced satisfactory efficiency (74%) and R^2 values (>0.99).

Amplicon Sequencing and Bioinformatics

Amplicon libraries were prepared, as per Illumina instructions by a 25-cycle PCR. PCR primers were the same as those used for qPCR but flanked with Illumina overhang sequences. A unique combination of Nextera XT v2 Indices (Illumina) were added to PCR products from each sample, via an 8-cycle PCR. PCR products were quantified using Quant-iT PicoGreen dsDNA Assay Kit (TheromFisher Scientific) and pooled in equimolar concentrations. Quantification of the amplicon libraries was determined via NEBNext® Library Quant Kit for Illumina (New England BioLabs Inc.), prior to sequencing on the Illumina MiSeq® platform, using a MiSeq® 600 cycle v3 reagent kit and 20% PhiX sequencing control standard. Sequence output from the Illumina MiSeq platform were analysed within BioLinux (Field *et al.*, 2006), using a bioinformatics pipeline as described by Dumbrell *et al.*, (2016). Forward sequence reads were quality trimmed using Sickle (Joshi and Fass, 2011) prior to error correction within SPades (Nurk *et al.*, 2013) using the BayesHammer algorithm (Nikolenko *et al.*, 2013). The quality filter and error corrected sequence reads were dereplicated, sorted by abundance, and clustered into OTUs (Operational Taxonomic Units) at the 97% level via VSEARCH (Rognes *et al.*, 2016). Singleton OTUs were discarded, as well as chimeras using reference-based chimera checking with UCHIME (Edgar *et al.*, 2011). Taxonomic assignment was conducted with RDP Classifier (Wang *et al.*, 2007). Non locus-specific, or artefactual, OTUs were discarded prior to statistical analyses, along with any OTUs that had <70% identity with any sequence in the RDP database.

Statistical Analysis

Data were first tested for normality (Shapiro-Wilks test), those data which were normally distributed were tested for significance with ANOVAs or appropriate linear models. Non-normally distributed data were analysed using appropriate GLMs (Generalised Linear Models) as follows. The relative abundance of OTUs or genera in relation depth, treatment, or time were modelled using multivariate negative binomial GLMs (Wang *et al.*, 2010). Here, the number of sequences in each library was accounted for using an offset term, as described previously (Alzarhani *et al.*, 2019). The abundance of bacterial 16S rRNA gene copies was also modelled using negative binomial GLMs (Venables and Ripley, 2002). The significance of model terms was assessed via likelihood ratio tests. The Environmental Index of Hydrocarbon Exposure (Lozada *et al.*, 2014) was calculated using the script available at the ecolFudge GitHub page (https://github.com/Dave-Clark/ecolFudge, Clark, 2019) and EIHE values modelled using poisson GLMs. All statistical analyses were carried out in R3.6.1 (R Development Core Team, 2011) using a variety of packages available through the references (Searle *et al.*, 1980; Venables and Ripley, 2002; Becker *et al.*, 2016; Auguie, 2017). All plots were constructed using the “ggplot2” (Bodenhofer *et al.*, 2011) and “patchwork” (Pedersen, 2019) R packages.

Results

Background bacterial 16S rRNA gene abundance in the surface of seawater was 86,293 (± 44,098) copies per ml of seawater, at 1.5 meters this was 98,438 (± 23,383) copies per ml of seawater, and at 5 meters was 84,725 (± 25,164) copies per ml of seawater (Fig. 1). Whilst there were no statistically significant results in the absolute abundance of bacterial copies, there are some temporal trends observed whereby a reduction is observed after 24 hours across all depths. With an average of 55% reduction at surface, 82% reduction at 1.5 meters, and 21% reduction at 5 meters in background bacterial gene copies. There are no observable significant differences between treatments.

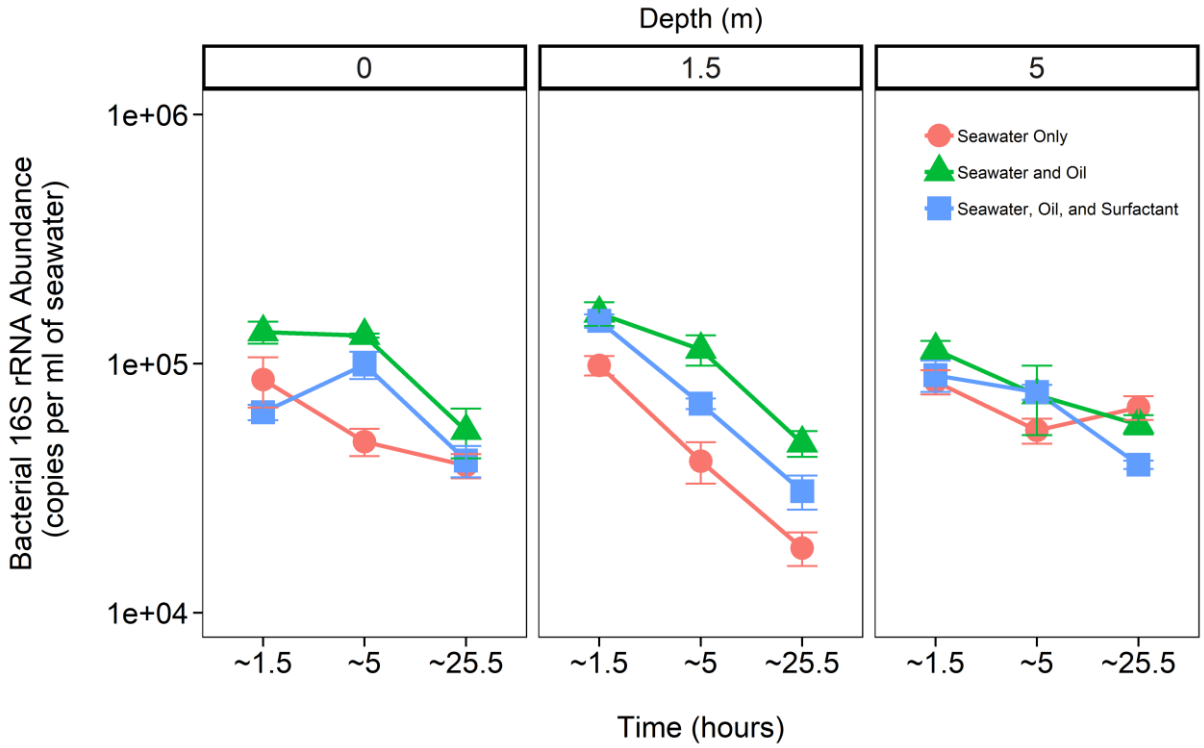

Fig 1: Bacterial 16S rRNA gene abundance (mean ± SE, *n* = 3) ~1.5 hours, ~5 hours, and ~ 25.5 hours after oil deposition. Measured within three treatments (Seawater Only, Seawater and Oil, and Seawater, Oil and Slickgone NS Dispersant) at surface level (0) and depths of 1.5 and 5 meters.

Temporal selection demonstrated the largest effect on the bacterial community composition (Fig. 2; R^2 = 0.28, F = 15.90, P<0.001) with depth and treatment demonstrating no significant effect (P>0.05).

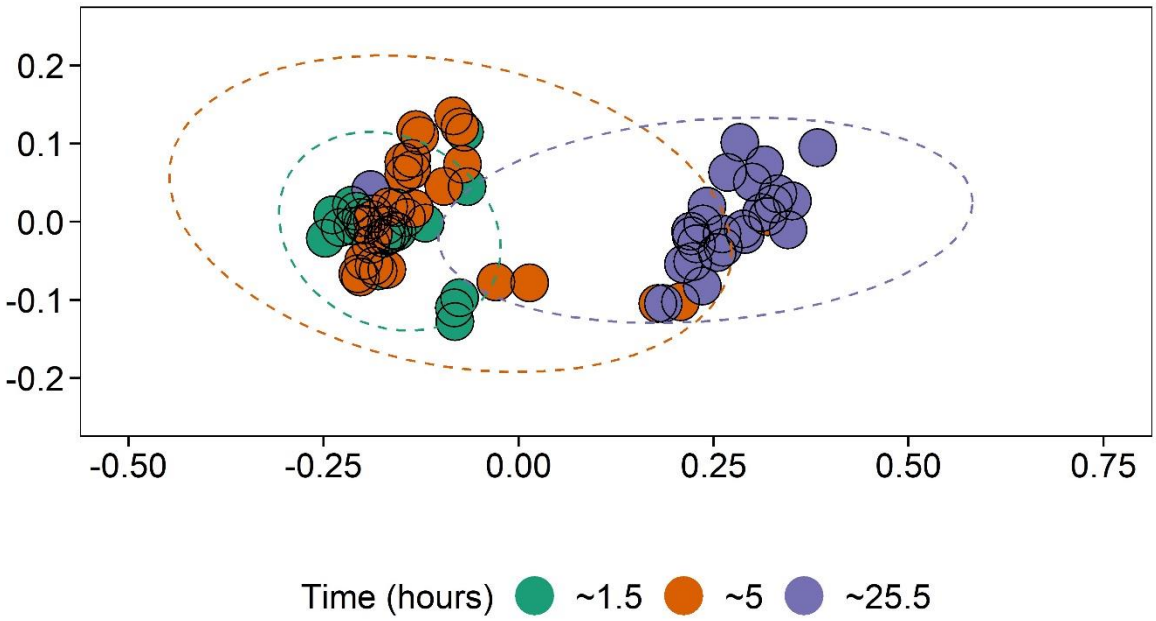

Fig. 2: NMDS (non-metric multidimensional scaling) ordination, based on clustered bacterial 16S rRNA OTUs at a 97% confidence level, displaying the effect of time (hours) on bacterial community composition (R^2 = 0.28, F = 15.90, P<0.001).

Whilst there was little effect on the overall community composition between treatments, based on preliminary analysis, some operational taxonomic units (OTUs) did demonstrate differences (Fig. 3). Most notably are the OTUs assigned to *Candidatus Pelagibacter* spp. and *Plankomarina* spp. (Fig. 3). OTU1, assigned to *Candidatus Pelagibacter* spp., represented the most abundant OTU in the bacterial 16S rRNA amplicon library. Approximately 24 hours after initial sampling, both treatments that contained oil demonstrated a significant decrease in relative abundance of OTU1 (coef. -6.02, z -3.53, P<0.05). Though at approximately 5 hours the treatment with Oil and Slickgone NS maintained significantly increased relative abundance in comparison to seawater only (coef. 7.07, z 4.15, P<0.01). At both 1 hour after oil deposit and 24 hours after initial sampling, the relative abundance of OTU4, assigned to *Plankomarina* spp., remained similar between all treatments. However, approximately 5 hours after oil deposit, whilst OTU4 had increased to 7% in the seawater control, this growth was significantly (coef. -4.18, z -9.19, P<0.001) inhibited in the treatment containing only oil (4.43 ± 0.51%) and more so with oil and Slickgone NS (2.94 ± 0.34%).

Analysis of bacterial 16S rRNA OTU sequences as a function of the Ecological Index of Hydrocarbon Exposure (Lozada *et al.*, 2014) revealed no significant differences between treatments, time points, or depths (Fig. 4). Moreover, with the index averaging less than 0.02, and the relative abundance of Obligate Hydrocarbonclastic Bacteria (OHCB) less than 1*10-6, it revealed the oil (with or without Slickgone NS) treatments did not promote the growth of oil-degrading bacteria within approximately 25 hours. This is likely due to the sampling not capturing the oil/water interface efficiently.

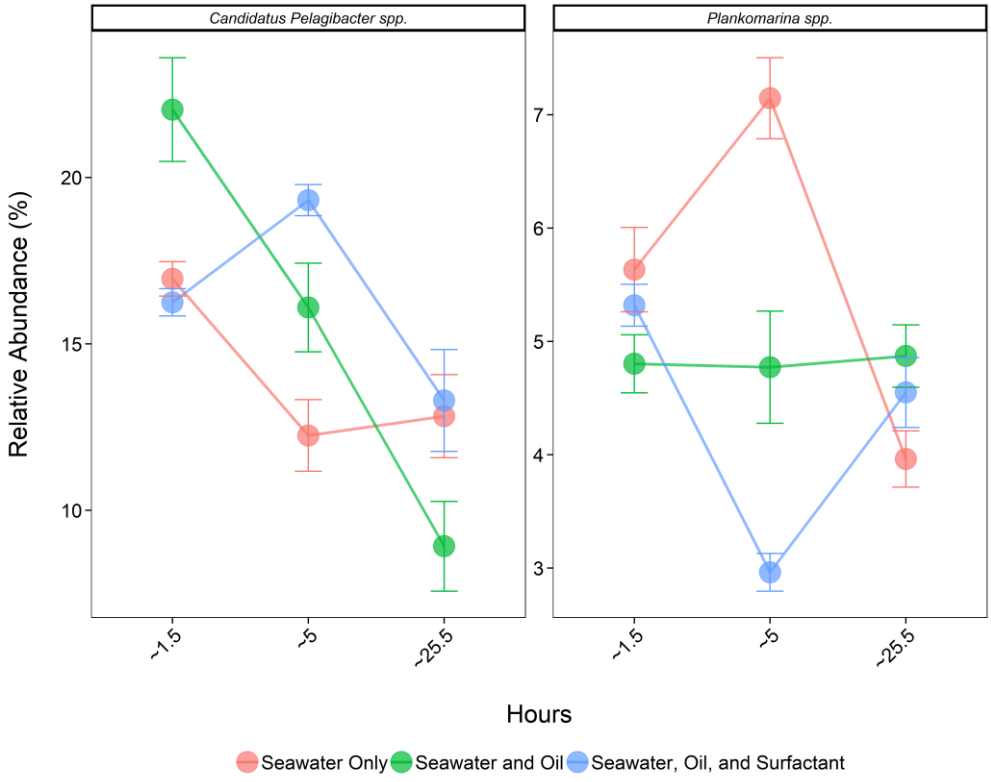

Fig. 3: Relative abundance (% of the bacterial community; mean ± SE, *n* = 3) of bacterial 16S rRNA gene, of OTUs belonging to the genera *Candidatus Pelagibacter* spp., and *Plankomarina* spp. ~1.5 hours, ~5

hours, and ~ 25.5 hours after oil deposition. Measured within three treatments (Seawater Only, Seawater and Oil, and Seawater, Oil and Slickgone NS Dispersant).

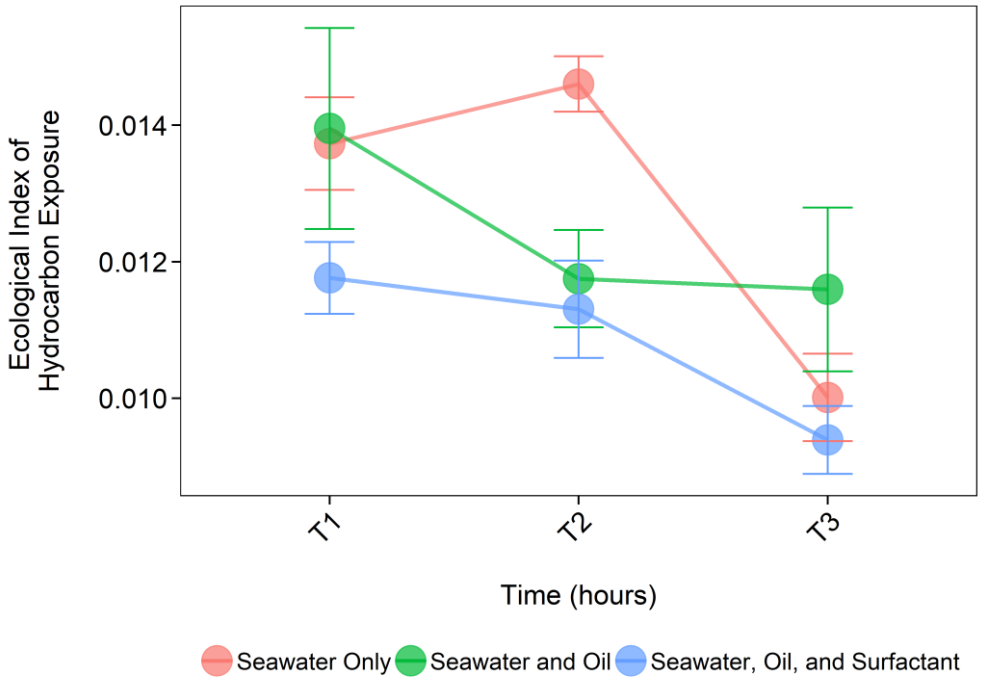

Fig. 4: Mean Environmental Index of Hydrocarbon Exposure (ratio %) representing relative abundance of Bacteria with hydrocarbon bioremediation potential (Lozada et al., 2014; mean ± SE, *n* = 3). ~1.5 hours (T1), ~5 hours (T2), and ~ 25.5 hours (T3) after oil deposition. Measured within three treatments (Seawater Only, Seawater and Oil, and Seawater, Oil and Slickgone NS Dispersant).

Analysis of nutrients (Fig. 5) revealed no significant difference between treatments 1 hour after the oil-slicks were released; with total N concentrations ranging from 8.45 – 9.37 µMol. Approximately 5.5 hours after oil-slick deposits, total N tended to decrease across all treatments, with ammonia (coef. -0.42, z -3.98, P<0.01) and nitrate (coef. -9.09, z -3.42, P<0.05) significantly decreased in the treatment containg oil and surfactant in comparison to oil only treatment. Approximately 25.5 hours after oil-slick deposits, total N significantly (coef. -14.70, z -5.42, P<0.001) decreased across all treatments from both other time points, to a range of 1.51 – 1.77 µMol. Phospherous was undetecable across all treatments and at all time points.

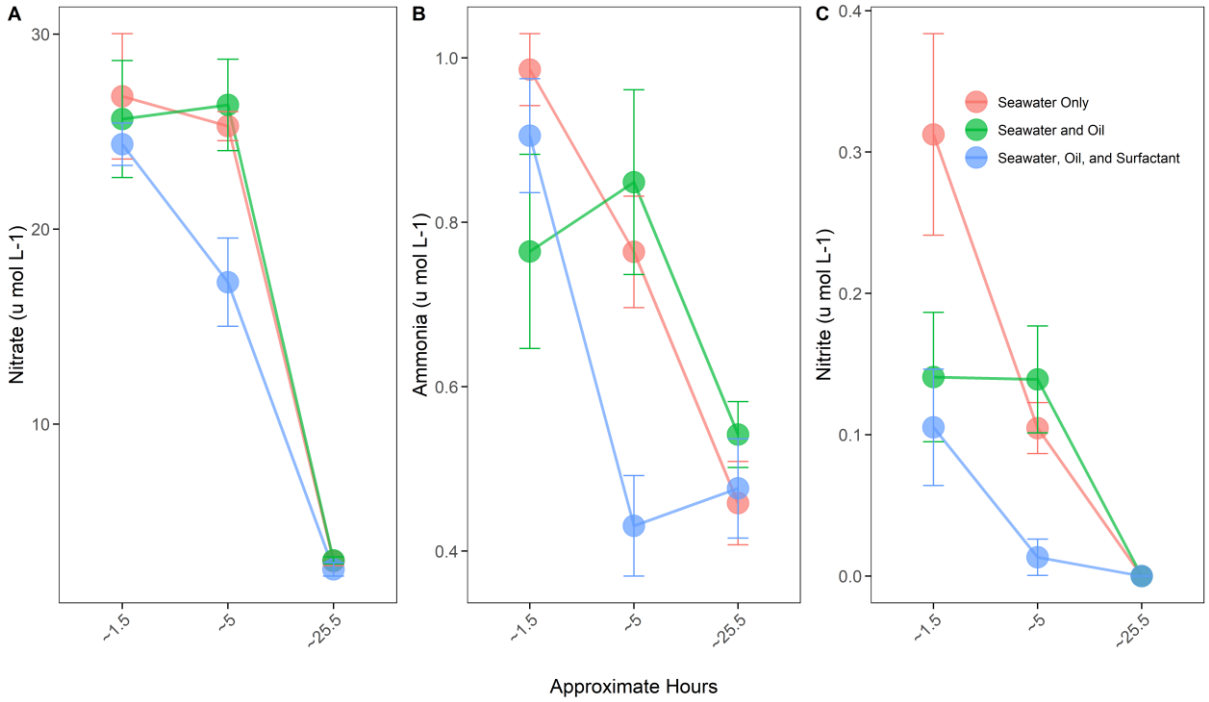

Fig. 5: Nitrate (A), ammonia (B), and nitrite (C) concentrations (mean ± SE, *n* = 3) from samples taken ~1.5 hours, ~5 hours, and ~ 25.5 hours after oil-deposition. Measured within three treatments (Seawater Only, Seawater and Oil, and Seawater, Oil and Slickgone NS Dispersant).

Apart from two samples no hydrocarbons were measured in sampled seawater. This further reflects the fact the sampling methodology did not capture the oil/water interface. The samples which did have measurable hydrocarbons were taken from the surface in the oil and Slickgone NS treatment ("Charlie") after 25.5 hours. Measurable hydrocarbons included an average concentration of *n*-alkanes (C^{14}-C^{31}) 188.13 (± 76.91) µg ml^{-1} seawater, branched alkanes (pristane and phytane) 27.20 (± 11.91) µg ml^{-1} seawater, and PAHs (phenanthrene and 2methyl-anthracene) 5.84 (± 3.13) µg ml^{-1} seawater.

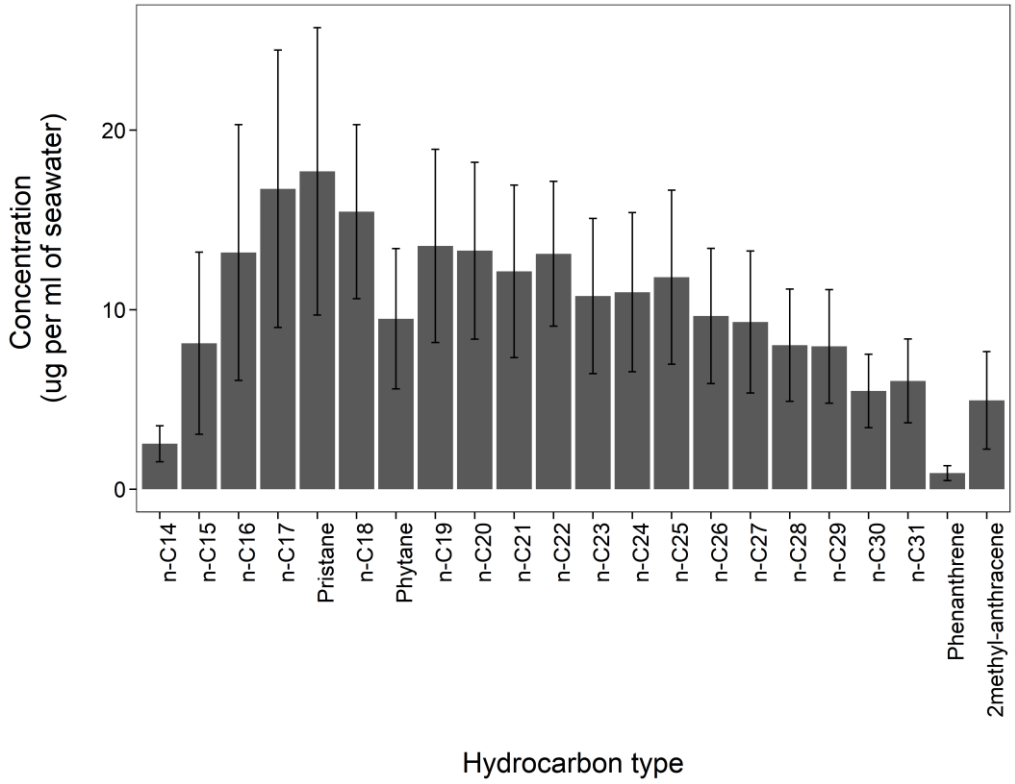

Fig. 6: Seawater samples taken from the "Oil and Slickgone NS" treatment ("Charlie") after 25.5 hours. Measured hydrocarbon concentrations (mean ± SE, *n* = 2) include *n*-alkanes (C^{14} to C^{31}), branched alkanes pristane and phytane, and PAHs (phenanthrene and 2-methyl-anthracene).

References

Alzarhani, A.K., Clark, D.R., Underwood, G.J.C., Ford, H., Cotton, T.E.A., and Dumbrell, A.J. (2019) Are drivers of root-associated fungal community structure context specific? *ISME J* **13**: 1330–1344.

Auguie, B. (2017) gridExtra: functions in Grid graphics. R Package Version 2.3. *CRAN Proj*.

Becker, R.A., Wilks, A.R., Brownrigg, R., Minka, T.P., and Deckmyn, A. (2016) Package "maps": Draw Geographical Maps. *R Packag version 23-6*.

Bodenhofer, U., Kothmeier, A., and Hochreiter, S. (2011) Apcluster: An R package for affinity propagation clustering. *Bioinformatics* **27**: 2463–2464.

Clark, D.R. (2019) ecolFudge.

Coulon, F., McKew, B.A., Osborn, A.M., McGenity, T.J., and Timmis, K.N. (2007) Effects of temperature and biostimulation on oil-degrading microbial communities in temperate estuarine waters. *Environ Microbiol* **9**: 177–186.

Dumbrell, A.J., Ferguson, R.M.W., and Clark, D.R. (2016) Microbial Community Analysis by Single-Amplicon High-Throughput Next Generation Sequencing: Data Analysis – From Raw Output to Ecology. In *Hydrocarbon and Lipid Microbiology Protocols*. McGenity, T.J., Timmis, K.N., and Nogales, B. (eds). Berlin, Heidelberg, Heidelberg: Springer Protocols Handbooks, pp. 155–206.

Edgar, R.C., Haas, B.J., Clemente, J.C., Quince, C., and Knight, R. (2011) UCHIME improves sensitivity and speed of chimera detection. *Bioinformatics* **27**: 2194–2200.

Field, D., Houten, S., Thurston, M., Swan, D., Tiwari, B., Booth, T., and Bertrand, N. (2006) Open software for biologists: from famine to feast. *Nat Biotechnol*.

Joshi, N. and Fass, J. (2011) sickle - A windowed adaptive trimming tool for FASTQ files using quality. *(Version 133)* [Software].

Klindworth, A., Pruesse, E., Schweer, T., Peplies, J., Quast, C., Horn, M., and Glöckner, F.O. (2013) Evaluation of general 16S ribosomal RNA gene PCR primers for classical and next-generation sequencing-based diversity studies. *Nucleic Acids Res* **41**: 1–11.

Lozada, M., Marcos, M.S., Commendatore, M.G., Gil, M.N., and Dionisi, H.M. (2014) The Bacterial Community Structure of Hydrocarbon-Polluted Marine Environments as the Basis for the Definition of an Ecological Index of Hydrocarbon Exposure. *Microbes Environ* **29**: 269–276.

McKew, B.A. and Smith, C.J. (2015) Real-Time PCR Approaches for Analysis of Hydrocarbon-Degrading Bacterial Communities. In *Hydrocarbon and Lipid Microbiology Protocols*. McGenity, T.J., Timmis, K.N., and Fernandez, B.N. (eds). Berlin, Heidelberg: Springer Protocols Handbooks.

Nikolenko, S.I., Korobeynikov, A.I., and Alekseyev, M.A. (2013) BayesHammer: Bayesian clustering for error correction in single-cell sequencing. *BMC Genomics* **14**:.

Nurk, S., Bankevich, A., Antipov, D., Gurevich, A., Korobeynikov, A., Lapidus, A., et al. (2013) Assembling genomes and mini-metagenomes from highly chimeric reads. In *Lecture Notes in Computer Science (including subseries Lecture Notes in Artificial Intelligence and Lecture Notes in Bioinformatics)*. pp. 158–170.

Pedersen, T.L. (2019) patchwork: The Composer of Plots. *Cran*.

R Development Core Team, R. (2011) R: A Language and Environment for Statistical Computing.

Rognes, T., Flouri, T., Nichols, B., Quince, C., and Mahé, F. (2016) VSEARCH: a versatile open source tool for metagenomics. *PeerJ* **4**: e2584.

Salisbury, D.J., Anguelova, M.D., and Brooks, I.M. (2014) Global distribution and seasonal dependence of satellite-based whitecap fraction. *Geophys Res Lett* **41**: 1616–1623.

Searle, S.R., Speed, F.M., and Milliken, G.A. (1980) Population marginal means in the linear model: An alternative to least squares means. *Am Stat* **34**: 216–221.

Tatti, E., McKew, B.A., Whitby, C., and Smith, C.J. (2016) Simultaneous dna-rna extraction from coastal sediments and quantification of 16S rRNA genes and transcripts by real-time PCR. *J Vis Exp* **2016**: e54067.

Venables, W.N. and Ripley, B.D. (2002) Modern Applied Statistics with S (Fourth Edition).

Wang, Q., Garrity, G.M., Tiedje, J.M., and Cole, J.R. (2007) Naïve Bayesian classifier for rapid assignment of rRNA sequences into the new bacterial taxonomy. *Appl Environ Microbiol* **73**: 5261–5267.

Wang, W., Wang, L., and Shao, Z. (2010) Diversity and Abundance of Oil-Degrading Bacteria and Alkane Hydroxylase (alkB) Genes in the Subtropical Seawater of Xiamen Island. *Microb Ecol* **60**: 429–439.

Zeinstra-Helfrich, M., Koops, W., and Murk, A.J. (2017) Predicting the consequence of natural and chemical dispersion for oil slick size over time. *J Geophys Res Ocean* **122**: 7312–7324.

Acute toxicity of oil and dispersed oil in water to a temperate amphipod

van den Heuvel-Greve, Martine J; de Vlieger, O; Abbenis, S; Murk, Albertinka J

Abstract

To assess the acute toxicity of water directly below the two oil slicks, water samples from the field tests were tested with the marine amphipod, *Gammarus locusta* at 9°C. No toxicity was observed after five days of exposure. Additionally worst case standard toxicity tests were conducted with the same oil and oil dispersed with the same dispersant as used in the field tests. Oil in water fractions were prepared by stirring floating oil on water for 48 hrs in a closed glass jar in the dark. The average LC50 value of these standard toxicity tests with *G. locusta* were 0.13 ml oil/L for Arabian light crude oil and 0.11 ml oil/L for Arabian light crude oil dispersed with SLICKGONE NS (in a 1:25 dispersant:oil ratio based on volume), resulting in a slightly enhanced toxicity of the dispersed oil (factor 1.2) compared to the non-dispersed oil. Comparison of the field tests with the standard laboratory tests showed that the field samples contained oil in water concentrations below the No Observed Effect Concentration for both the oil and the dispersed oil.

Materials & Methods

Test species

Toxicity tests were conducted using the epibenthic marine amphipod, *Gammarus locusta* (Costa et al., 1998). *G. locusta* is widely spread along the European Atlantic coast and can be found in Portugal, all the way up to Iceland (Lincon, 1979). The species is mostly abundant in high salinity areas but can prevail in brackish waters as well (Costa et al., 1998; Costa & Costa, 1999). They can be found from the intertidal zone to a depth of 30 meters (Hartog den, 1963; Costa et al., 1998; Costa & Costa, 1999).

Individual *G. locusta* were collected from the wild. They were collected 1-5 days prior to each experiment. Collection took place in an intertidal area in the Dutch Oosterschelde near Goese Sas (51°32’43.36”N; 3°55’28.79”E). Gammarids were collected in the period from February till April 2019, and kept in an aquarium at test temperature until the start of the tests. They were fed with Tetra Wafer MiniMax food prior to the test. Species ranging from 6-15 mm in length were selected for testing.

Test chemicals

The tested oil was Arabian light crude oil (after 48 hrs of stirring, see below) and the applied dispersant was SLICKGONE NS, and identical to the oil and dispersants used in the field experiments.

Laboratory tests

Toxicity tests were performed in the laboratory to assess the LC50 value for both the oil and dispersed oil, during February-April 2019 (prior to the field test). The tests were executed with water-accommodated fractions of both the oil (WAF) and the dispersed oil (the chemically enhanced water-accommodated fractions - CEWAF). The WAF and CEWAF were prepared with artificial seawater (ASW) using Pro Reef Salt Mix (Colombo®) mixed with Milli-Q water to obtain a salinity of 34-36‰, which is comparable to Oosterschelde seawater.

WAF and CEWAF preparation took place in a climate room in 5L glass Duran® bottles. First 5.2 L of ASW was added to each of the bottles. Then oil or oil and dispersant was added to each of the

bottles. The concentration of dispersant was 1:25 dispersant:oil ratio based on volume. The ASW in combination with oil, or oil and dispersant was stirred for 48 hour using a stir bar and a stir plate. The test temperature was measured for test weeks 6-12 using a temperature logger placed in a water bottle. The average test temperature was 9.34˚C ±0.38 (based on test weeks 6-12), which was comparable to the temperature of the field experiment (see 2.1.4.).

A set of eight bottles with individually dosed concentrations were tested during each test. Increasing concentrations were added to each of these bottles to be able to draft a concentration curve (Tables 2A/2B). A range finding test was conducted first to get a first indication of the oil's toxicity prior to the ultimate tests.

Table 2A. Nominal oil concentrations used in the toxicity studies with Arabian light crude oil during subsequent Test Weeks (TW).

		TW0	TW1	TW2	TW3	TW4
Tx	Oil (ml/L)	Range Finding	LC_{50} Oil	LC_{50} Oil	LC_{50} Oil	LC_{50} Oil
C0	0	x	x	x	x	x
C0d	0					
C1	0.001	x				
C1,5	0.002					
C2	0.003		x	x		
C3	0.010	x	x	x	x	
C3,5	0.019					
C4	0.029		x	x	x	x
C4,5	0.067			x	x	x
C4.7	0.081					
C5	0.096	x	x	x	x	x
C5,2	0.125					x
C5,4	0.163					x
C5,5	0.192				x	x
C6	0.288		x	x	x	x
C7	0.962	x	x	x	x	
C8	2.88		x			
C9	9.62	x				

Table 2B. Nominal oil and dispersant concentrations used in the toxicity studies with Arabian light crude oil and the dispersant SLICKGONE NS.

			TW5	TW6	TW7
Tx	Oil (ml/L)	Dispersant (ml/L)	LC_{50} Dispersed Oil	LC_{50} Dispersed Oil	LC_{50} Dispersed Oil
C0	0	0	x	x	x
C0d	0	0.012	x	x	x
C1	0.001	0.00004	x		
C1,5	0.002	0.00008	x		
C2	0.003	0.00012			
C3	0.010	0.00038	x		
C3,5	0.019	0.00077	x		
C4	0.029	0.001		x	x
C4,5	0.067	0.003		x	x
C4.7	0.081	0.003			x
C5	0.096	0.004	x	x	x
C5,2	0.125	0.005		x	x
C5,4	0.163	0.007			
C5,5	0.192	0.008	x	x	x
C6	0.288	0.012	x	x	
C7	0.962	0.038			
C8	2.885	0.115			
C9	9.615	0.385			

After 48 hrs of stirring the WAF of each 5L bottle was gently poured into five 1L glass test bottles at low light, allowing five replicates per concentration. Gammarids (n=8) were added to each 1L glass beaker containing WAFs. Every test contained one set of controls (n=5) to ensure that test species were only adversely affected by the toxic compounds. After addition of the Gammarids, the test bottles were sealed with hexane-rinsed aluminum foil to reduce evaporation and photo degradation. Oxygen levels were measured prior to and at the end of each test using a Hach© HQ-40d multimeter with an LDO probe. At the start of the test, one test bottle of each concentration was used to measure the oxygen concentration representing the oxygen levels for all test bottles of that specific concentration. At the end of the test, oxygen levels were measured in all replicates of the test bottles.

Gammarid survival was scored every 24 hours, for five days. The obtained mortality data was recorded, used to create dose-response curves and to determine the LC50 values. Dose-response curves were obtained by log transforming the acquired dose data.

Testing continued until at least two test weeks were defined as sufficient for each of the tests. A test week defined as ‘sufficient’ met the following requirements: (1) a maximum of 10% mortality in the blanc (C0); (2) at least one concentration with no mortality (C0 excluded); (3) at least one concentration with 100% mortality; and (4) at least two or more concentrations with a mortality higher than 0% and lower than 100%. In total, 12 test weeks were conducted (Table 3). Of these,

TW3 and TW4 were rated 'sufficient' for the oil WAF toxicity tests and TW6 and TW7 for the dispersed oil CEWAF toxicity tests.

Concentrations reported here are nominal, meaning the volume of oil that was added, not the actual chemical concentrations of the oil components in water (WAF/CEWAF). These actual concentration will be analysed at a later stage. For this purpose ~450 ml of each WAF/CEWAF was stored in 500 ml amber coloured bottles containing 50 mL n-Hexane (Biosolve B.V., Netherlands). The bottles were stored in the climate room at 9°C until transport to the University of Essex.

Table 3: Total of all tests that were conducted to assess the toxicity of WAF and CEWAF of Arabian Crude light oil. 'Sufficient' was allocated based on quality criteria of the tests.

Test week #	**Abbreviation**	**Focus**	**Sufficient**
Test week 0 - range finding	TW0	Oil	No
Test week 1	TW1	Oil	No
Test week 2	TW2	Oil	No
Test week 3	TW3	Oil	Yes
Test week 4	TW4	Oil	Yes
Test week 5	TW5	Dispersed Oil	No
Test week 6	TW6	Dispersed Oil	Yes
Test week 7	TW7	Dispersed Oil	Yes
Test week 8	TW8	Dispersant only	No
Test week 9	TW9	Dispersant only	No
Test week 10	TW10	Dispersant only	No
Test week 11	TW11	Field Test	Yes
Test week 12	TW12	Dispersant only	No

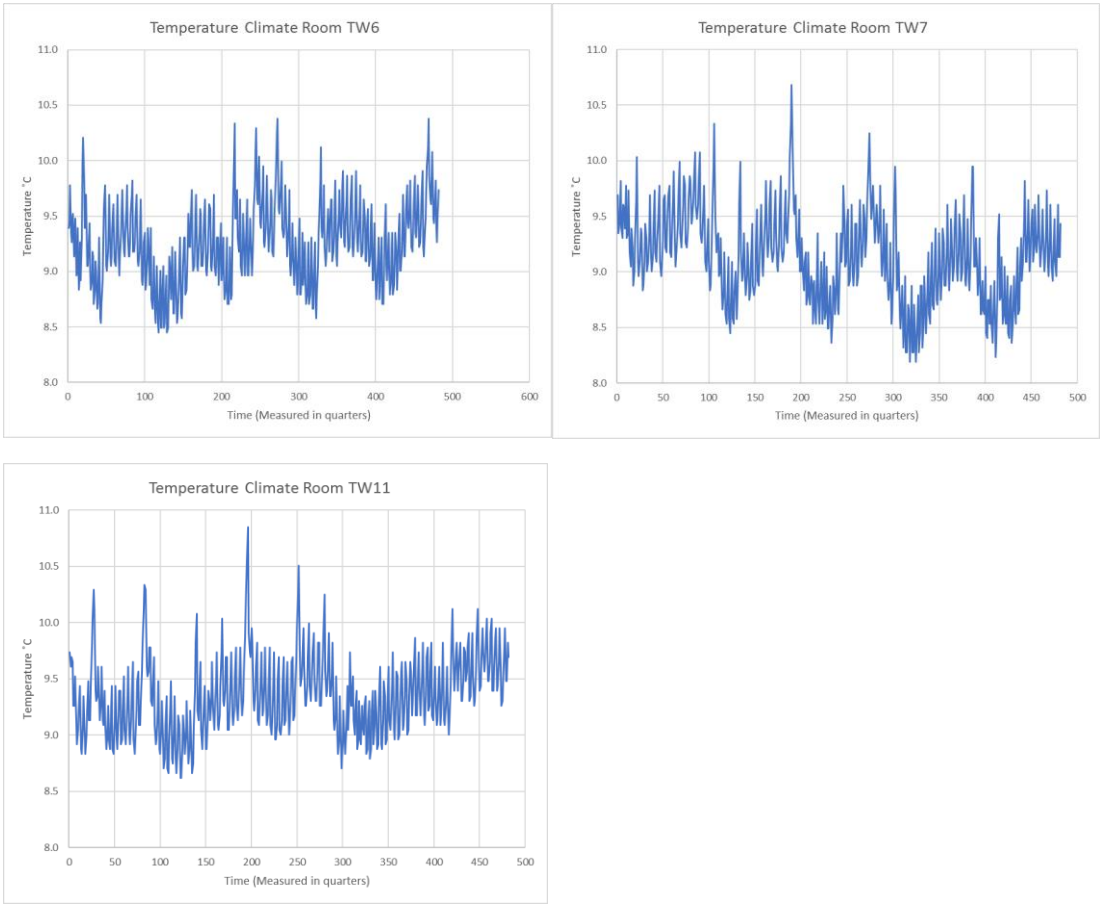

Figure 18. Test temperature of test weeks 6 (Panel A: 9.26˚C ±0.36), 7 (Panel B: 9.14˚C ±0.42) and 11 (Panel C: 9.36˚C ±0.35). No temperature data were available for test weeks 3 and 4. See Table 2 for details on the test weeks. Average test temperature of weeks 6-12 was 9.34˚C ±0.38.

Field test

Field samples were collected during the oil spill field experiment. Each oil slick contained three sample locations; (1) a sample taken in the middle of the slick, at a depth of 1.5 meters, (2) a sample taken in the middle of the slick, at a depth of 5 meters and (3) a sample outside the oil slick, to serve as blanc, at a depth of 1.5 meters. For each sample, three replicates were collected and samples were collected at T1 and T2 for the oil toxicity tests (table 4).

The actual LC50 experiments were conducted at a later time (test week 11). Field samples were stored at -20˚C in the dark until they were tested, to prevent any further weathering of the samples during storage. The samples were slowly melted prior to testing by placing them for 36 hours at test temperature (~9˚C). When the samples reached test temperature, eight individual gammarids were directly placed in each of the sample jars and the test was completed as described above for the 5-day toxicity test.

Data analysis

Dose response curves were created to determine the LC50 of the Arabian light crude oil and the dispersed Arabian light crude oil using Graphpad Prism 8. Data was processed and analysed by executing a non-linear regression.

Table 4. Details on collected water samples from the field experiment, that were provided by the sampling team, to test for oil toxicity using *G. locusta*.

#	Sample code	Date	Time	Coordinate	Coordinate	Slick	Sample position in slick	T1/T2	Depth	Replicate
	on sample jars					*Bravo - Charlie*	*In - out*	*T1 - T2*	*1.5 - 5 m*	*1 - 2 - 3*
1	Bravo T1 1.5C 1	16/apr/19				Control	Out	T1	1.5	1
2	Bravo T1 1.5C 2	16/apr/19				Control	Out	T1	1.5	2
3	Bravo T1 1.5C 3	16/apr/19				Control	Out	T1	1.5	3
4	Bravo T1 1.5 1	16/apr/19	11:35	52°14'52,9"N	3°57'17,5"E	Bravo	In	T1	1.5	1
5	Bravo T1 1.5 2	16/apr/19	11:35	52°14'52,9"N	3°57'17,5"E	Bravo	In	T1	1.5	2
6	Bravo T1 1.5 3	16/apr/19	11:35	52°14'52,9"N	3°57'17,5"E	Bravo	In	T1	1.5	3
7	Bravo T1 5 1	16/apr/19	11:35	52°14'52,9"N	3°57'17,5"E	Bravo	In	T1	5	1
8	Bravo T1 5 2	16/apr/19	11:35	52°14'52,9"N	3°57'17,5"E	Bravo	In	T1	5	2
9	Bravo T1 5 3	16/apr/19	11:35	52°14'52,9"N	3°57'17,5"E	Bravo	In	T1	5	3
10	Charlie T1 1.5 1	16/apr/19	13:46	52°18'56,3"N	3°56'21,3"E	Charlie	In	T1	1.5	1
11	Charlie T1 1.5 2	16/apr/19	13:46	52°18'56,3"N	3°56'21,3"E	Charlie	In	T1	1.5	2
12	Charlie T1 1.5 3	16/apr/19	13:46	52°18'56,3"N	3°56'21,3"E	Charlie	In	T1	1.5	3
13	Charlie T1 5 1	16/apr/19	13:46	52°18'56,3"N	3°56'21,3"E	Charlie	In	T1	5	1
14	Charlie T1 5 2	16/apr/19	13:46	52°18'56,3"N	3°56'21,3"E	Charlie	In	T1	5	2
15	Charlie T1 5 3	16/apr/19	13:46	52°18'56,3"N	3°56'21,3"E	Charlie	In	T1	5	3
16	Bravo T2 1.5C 1	16/apr/19				Control	Out	T2	1.5	1
17	Bravo T2 1.5C 2	16/apr/19				Control	Out	T2	1.5	2
18	Bravo T2 1.5C 3	16/apr/19				Control	Out	T2	1.5	3
19	Bravo T2 1.5 1	16/apr/19	14:42	52°20'09,7"N	3°57'40,3"E	Bravo	In	T2	1.5	1
20	Bravo T2 1.5 2	16/apr/19	14:42	52°20'09,7"N	3°57'40,3"E	Bravo	In	T2	1.5	2
21	Bravo T2 1.5 3	16/apr/19	14:42	52°20'09,7"N	3°57'40,3"E	Bravo	In	T2	1.5	3
22	Bravo T2 5 1	16/apr/19	14:42	52°20'09,7"N	3°57'40,3"E	Bravo	In	T2	5	1
23	Bravo T2 5 2	16/apr/19	14:42	52°20'09,7"N	3°57'40,3"E	Bravo	In	T2	5	2
24	Bravo T2 5 3	16/apr/19	14:42	52°20'09,7"N	3°57'40,3"E	Bravo	In	T2	5	3
25	Charlie T2 1.5 1	16/apr/19	17:01	52°24'41,3"N	4°01'16,1"E	Charlie	In	T2	1.5	1
26	Charlie T2 1.5 2	16/apr/19	17:01	52°24'41,3"N	4°01'16,1"E	Charlie	In	T2	1.5	2
27	Charlie T2 1.5 3	16/apr/19	17:01	52°24'41,3"N	4°01'16,1"E	Charlie	In	T2	1.5	3
31	Charlie T2 5 1	16/apr/19	17:01	52°24'41,3"N	4°01'16,1"E	Charlie	In	T2	5	1
32	Charlie T2 5 2	16/apr/19	17:01	52°24'41,3"N	4°01'16,1"E	Charlie	In	T2	5	2
33	Charlie T2 5 3	16/apr/19	17:01	52°24'41,3"N	4°01'16,1"E	Charlie	In	T2	5	3

Results and discussion

LC50 value – oil

Test weeks 3 and 4 both showed a steep dose response curve indicating a rapid increasing toxicity of the tested oil (Figure 19). The corresponding LC50 values were 0,125 ml oil/L for TW3 and 0,127 ml oil/L for TW4. As both dose response curves (and corresponding LC50 values) were very similar, dose response values were combined, resulting in an averaged LC50 value of 0,126 ml oil/L for Arabian light crude oil (based on test weeks 3 & 4). The dispersant SLICKGONE NS did not show any signs of toxicity in the used concentrations as the highest concentrations were applied in additional blanks and no additional mortality was observed.

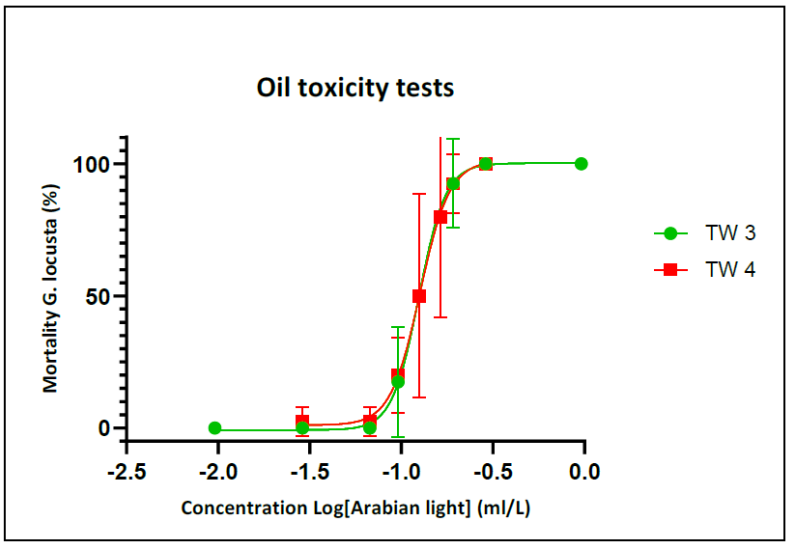

Figure 19. Dose response curves of *Gammarus locusta* exposed to different concentrations of Arabian light crude oil at 9˚C (test weeks 3 and 4). Concentrations are based on nominal values.

LC50 value – dispersed oil

Test week 6 and 7 (TW6 and TW7) produced steep dose response curves (figure 20). The LC50 values for Arabian light crude oil dispersed with SLICKGONE NS were 0.115 ml oil/L for TW6 and 0.100 ml oil/L for TW7. As the two test weeks showed similar values and trends, the two test weeks were combined to an averaged LC50 value for Arabian light crude oil dispersed with SLICKGONE NS of 0.105 ml oil/L (based on TW6 and TW7).

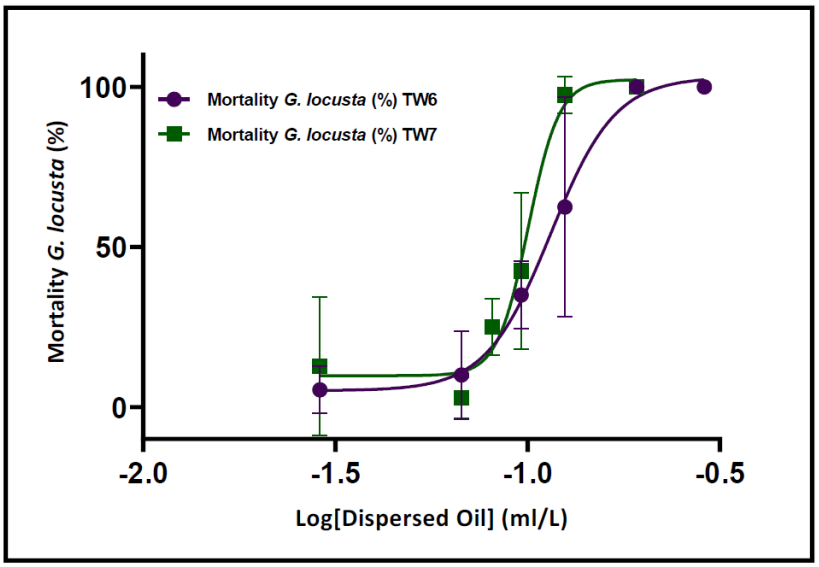

Figure 20. Dose response curves of *Gammarus locusta* exposed to different concentrations of dispersed oil based on Arabian light crude oil and SLICKGONE NS at 9˚C (test weeks 6 and 7). Concentrations are based on nominal values.

Comparison LC50 value – oil and dispersed oil

Averaged dose-response curves of Arabian light crude oil and Arabian light crude oil dispersed with SLICKGONE NS showed that the dispersed oil (0.105 ml oil/L) was slightly more toxic (factor 1.2 times) than non-dispersed oil (0.126 ml oil/L), when based on nominal concentrations (figure 21). Actual chemical concentrations will be determined, though results will be too late for incorporation in this report.

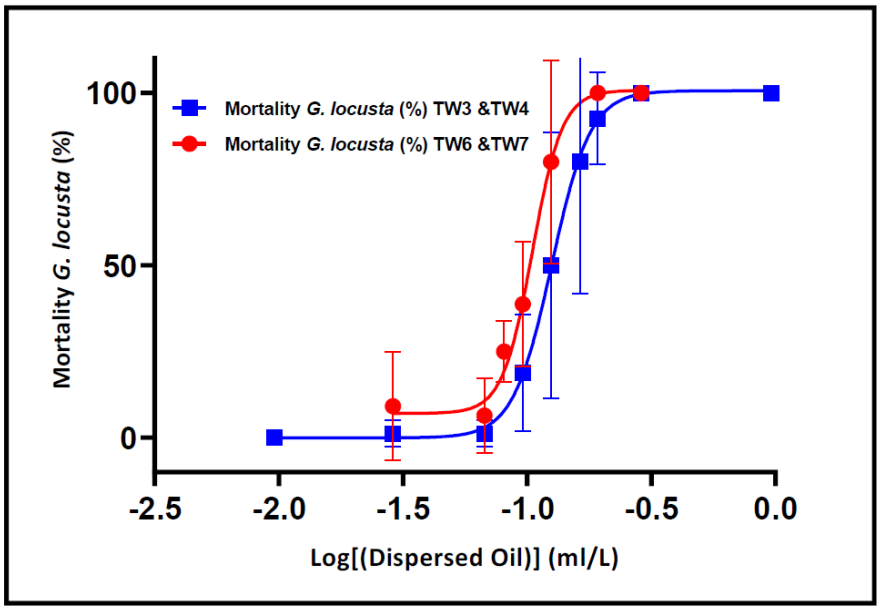

Figure 21. Dose response curves of *Gammarus locusta* exposed to different concentrations of Arabian light crude oil (based on TW3 & TW4) and Arabian light crude oil dispersed with SLICKGONE NS (based on TW6 & TW7) at 9˚C. Concentrations are based on nominal values.

Field test

Although a weak oil odour was noted in the water collected from the field experiment, the gammarids exposed to samples collected in the field showed a survival rate of 100%. Of all test organisms one individual died, in one of the control samples. This indicated that concentrations of oil in the field samples were similar to or lower than the No Observed Effect Concentrations (NOEC) of 0.03 ml oil/L and 0.002 ml oil/L for both oil and dispersed oil respectively. As the chemical analysis of the field samples have not been conducted yet, no further comparison with the laboratory tests can be made.

Laboratory tests were conducted in full darkness and with the prevention of evaporation, while the oil slicks in the field tests were influenced by evaporation, spreading, photo-oxidation and other relevant weathering processes that influence the presence of dissolved oil component in the water phase.

Discussion/Conclusion

Averaged LC50 values for *G. locusta* exposed for 5 days at 9˚C to Arabian light crude oil and Arabian light crude oil dispersed with SLICKGONE NS were 0.126 ml oil/L and 0.105 ml oil/L respectively, indicating that the dispersed oil was slightly more toxic (factor 1.2) than non-dispersed oil when based on nominal concentrations. Samples collected from the field during the field experiment with

Arabian light crude oil and Arabian light crude oil dispersed with SLICKGONE NS did not show mortality indicating that the oil concentrations in the field were at or below the No Observed Effect Concentrations (NOEC) for this oil type and dispersant.

Acknowledgements

Vincent Escaravage is thanked for organising the sampling of water during the field experiment.

References

Costa, F.O., Correia, A.D., Costa, M.H. (1998). Acute Marine Sediment Toxicity: A Potential New Test with the Amphipod *Gammarus locusta*. Ecotoxicology and Environmental Safety, 40(1-2), 81-87.

Costa, F.O., Costa, M.H. (1999). Life history of the amphipod *Gammarus locusta* in the Sado estuary (Portugal). Acta oecologica, 20(4), 305-314.

Hartog den, C. (1963). The amphipods of the deltaic region of the rivers Rhine, Meuse and Scheldt in relation to the hydrography of the area part II. The Talitridae. Netherlands Journal of Sea Research, 2(1), 40-67.

Lincoln R.J., British Marine Amphipoda: Gammaridea, British Museum (Natural History), London, 1979, 658 p.

4 Related laboratory studies

Brussaard, Corina (NIOZ/UvA) and Gianluca Bizzaro (NIOZ)

In collaboration with the WUR lab experiments were performed, whereby WUR focused mostly on floc formation after exposure with dispersant under different growth conditions and NIOZ tested sensitivity of phytoplankton to dispersant exposure as well as the effect of dispersant on virus-host interactions.

***Objective 1**: Test sensitivity of phytoplankton to exposure with dispersant: Corexit (earier used by WUR; Van Eenennaam et al. 2016) and Slickgone (used during the ExpOS'D spills).*

We successfully used 6 different phytoplankton species, representing major phytoplankton taxonomic groups in Dutch coastal waters. We furthermore tested mixed culture of different diatoms (WUR culture collection) but this one failed to grow consistently and was dismissed for further research. For both Corexit and Slickgone, seven concentrations ranging from 0.01 to 0.5 mL/L (final concentration) were tested against control cultures receiving medium instead of dispersant. Considering we also wanted to examine the effect of dispersant on virus-host interactions, we needed to make sure to find a dispersant concentration at which the two algal model species used were still alive as only living cells allow the production of virus progeny after infection. As expected, all control cultures grew well. The treated cultures, however, quickly showed a reduction in growth or even displayed cell death. The sensitivity to the dispersants differed by a factor 10 to 100 between the species tested. Despite a general sensitivity to high dispersant concentration exposure, the more detailed response does not seem to be general or even class-specific. High sensitivity of some species to very low concentrations of dispersant are still ecologically relevant as under natural conditions the dispersant is (rapidly) diluted by mixing.

***Objective 2**: Test at what concentration of dispersant (COREXIT and SLICKGONE) visible flocculation of the algal cultures occurs (extracellular polymer substances, EPS).*

All phytoplankton species tested for objective 1 were also used for objective 2 (exponentially growing, using glass tubes and settling columns). The tubes were only gently mixed the first day to accommodate larger floc formation over time. Cultures where visually monitored for two weeks; every hour for the first 8 h to check for potential immediate flocculation and thereafter once a day. In general, only high concentrations of dispersant were capable of inducing visible EPS flocs in the algal cultures. The two dispersants produced different type of flocs. At these concentrations, most phytoplankton species died. Using Corexit, flocs were often small, but eventually sank to the bottom of the tube. Earlier experiments with Dunaliella indicated floc formation (Van Eenennaam et al. 2016), however in our experiments Dunaliella did not show visual floc production (also not in a second trial with higher algal abundances). The response to dispersant exposure may be strain-specific.

***Objective 3**: To study how environmental relevant concentrations of two types of dispersants affect the host-virus interaction during the infection cycle.*

One-step infection cycle experiments were conducted using two virus-algal host model systems. Samples were taken for flow cytometric enumeration of algal cells and viruses. The non-infected cultures grew well during the experiment, and the non-treated infected cultures displayed a typical infection cycle. Upon addition of dispersant, species-specific responses were observed. There are, to our knowledge, no data published on the effect of dispersant on virus-host

dynamics despite the importance of viruses as mortality factor of phytoplankton (Mojica et al. 2016). We show that the use of dispersants can selectively impact viral lysis of phytoplankton. This will likely favor specific species over others, assuming other loss factors such as grazing, are not affected by dispersant exposure.

We are currently writing a scientific paper about this research, which will contain a more comprehensive description of the experiment and its results.

References

Mojica, K.D.A., Huisman, J., Wilhelm, S.W., Brussaard, C.P.D. (2016). Latitudinal variation in virus-induced mortality of phytoplankton across the North Atlantic Ocean. ISME Journal, 10, 500–513.

Van Eenennaam, J.S., Wei, Y., Grolle, K.C.F., Foekema, E.M., Tinka A.J. (2016). Oil spill dispersants induce formation of marine snow by phytoplankton-associated bacteria. Marine Pollution Bulletin, 104, 294-302.